Control of a multi-robot cooperative team guided by a human-operator

eingereichte
MASTERARBEIT
von

cand. ing. Martin Angerer

geb. am 10.06.1991
wohnhaft in:
Steinheilstrasse 5
80333 München
Tel.: 0151 57978548

Lehrstuhl für
INFORMATIONSTECHNISCHE REGELUNG
Technische Universität München

Univ.-Prof. Dr.-Ing. Sandra Hirche

Betreuer: Selma Musić, M.Sc.
Beginn: 01.10.2015
Zwischenbericht: 21.01.2016
Abgabe: 15.06.2016

In your final hardback copy, replace this page with the signed exercise sheet.

Abstract

Interaction between humans and robots in cooperative manipulation expands the range and complexity of admissible tasks. A shared control approach allows the user to teleoperate the overall formation, while the robots establish their coordination autonomously. Human-in-the-loop stability proofs in telemanipulation usually base on a dynamic model of the human arm manipulating a reactive input device.
In general the human behaviour is unknown and user interfaces, like gesture recognition or motion tracking, allow for possibly unstable or unsafe inputs. Without a model of the human behaviour, control design must ensure stability regardless the user's commands. The proposed model-based controller uses virtual structures to coordinate robot motion and virtually couples the human operator. The port-Hamiltonian formulation of the controller unveils its energetic state, which is used to adapt the (virtual) coupling of the operator. An energy tank passivates the coupling and limits the energy stored in the controlled system.
Human-in-the-loop stability and safety in teleoperation of a cooperative robot team using a non-reactive input interface is analysed for the first time. The control scheme is proven to be intrinsically passive and achieves stability with any user input. Collision safety for humans on-site is enhanced by the limited stored energy. Simulation results validate 1) the coordination preservation of the robots, 2) the overall trajectory following, 3) the energy-bounding of the controlled system.

Zusammenfassung

Die Interaktion von Menschen und kooperativ-arbeitenden Roboter erweitert das Spektrum möglicher Aufgaben. Geteilte Zuständigkeiten in der Regelung erlauben es dem Benutzer dei geschlossene Formation der Roboter zu fernzusteuern, während die Roboter die Formation selbstständig herstellen. Die Stabilität ferngesteuerter Roboter wird mittels physiologischer Modelle des menschlichen Arms bewiesen.
Allgemein ist das Verhalten des Menschen unbekannt und neuartige Benutzerschnittstellen wie eine Handgestensteuerung erlauben Kommandos die nicht von physiologischen Modellen beschrieben werden. Ohne ein Modell menschlicher Dynamik obliegt es dem Regler instabile oder gefährliche Eingaben auszuschließen. Der vorgeschlagene modellbasierte Regler koordiniert, mittels virtueller Strukturen, die Formation der Roboter und bindet den Benutzer virtuell ein. Der energetische Zustand des Reglers bestimmt die adaptive Kopplung des Benutzers. Ein Energiespeicher stellt eine passive Kopplung sicher und begrenzt die im Regler gespeicherte Energie.
Dies ist die erste Untersuchung der Stabilität kooperativ-arbeitender Roboter, die über eine nicht-restriktive Schnittstelle ferngesteuert werden. Der Regelansatz ist erwiesenermaßen passiv und stabil mit beliebigen Eingaben. Die Verletzungsgefahr bei einer Kollision wird durch Energiebegrenzung verringert. Simulationsergebnisse belegen 1) die automatische Koordination der Roboter, 2) das Folgeverhalten auf Kommandos, 3) die Energiebegrenzung des Systems.

Contents

Chapter 1

Introduction

Interaction between humans and robots expands the range and complexity of admissible tasks in a natural way: humans come with superior foresight and planning capabilities, while being inherently robust and adaptive in unexpected situations. On the other hand, robots perform tasks repetitively and with high precision. In addition, robots can operate in areas humans cannot (space, hazardous environments). Remote human control, i.e. teleoperation, of the robots combines human cognition with robotic strength. Multiple robots working together in a cooperative team are capable of carrying out more complex tasks with less specialized tools. The prime example is grasping and transportation of large and/or heavy objects. Other options are the coordinated use of tools and the assembly of multiple parts without using special fixtures [CM08].
For several teleoperated robots in a cooperative team a variety of feasible control topologies exists. Dependant on the role of the human in the control loop and the level of autonomy of the robotic team, three classes of architectures are distinguished: direct, shared and supervisory control [HB12]. In direct control approaches humans operate each robot separately by manipulating a haptic device, e.g. [Goe52]. On the other hand, applying supervisory control, the robotic teams act autonomously and the operator issues high-level commands, e.g. "relocate to a certain place" or "grasp an object" [PST+15]. The operator continuously receives information on the state of the robotic system and periodically issues commands, thus rather oversees and directs than controls the system [She92]. The intermediate between supervised and directly controlled systems are shared control systems. At least some local, low-level feedback loops refine the robot behaviour to assist the operator in high-level task execution [NPH08]. One natural evolution of shared control for multiple robots is the leader-follower paradigm. The leader (in our case the human user) is not physically coupled to the robotic team, but virtually directs the robotic followers. The formation of the robotic followers is established automatically (low-level task), thus the user can focus on guiding the closed formation (high-level task). In contrast to supervisory control the human is directly included in the control loop and her/his dynamic behaviour affects the overall stability.

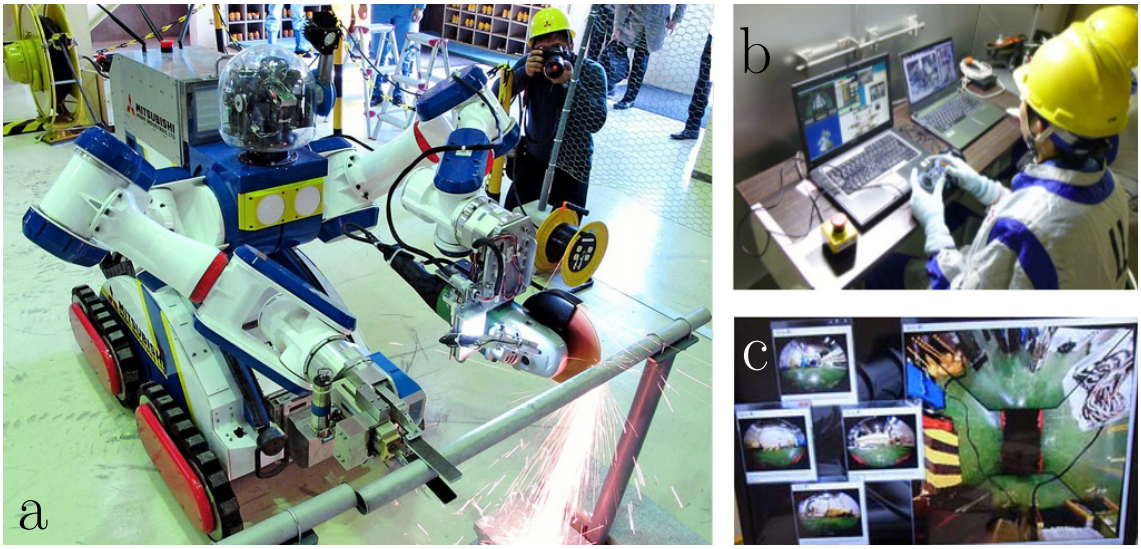

Figure 1.1: Demonstration of the teleoperated MHI MEISTeR robot at Fukushima Daiichi Nuclear Power Station [Ind14]: a) the robot carrying out a coordinated use of tools task b) operators using video game controllers c) visual feedback for the operator as displayed on the computer screen

The virtual integration of the human into the robotic set-up requires an interface that formalizes the indirect human-robot interaction. A common user interface in robotic teleoperation is the master-slave relation. The master-device is manipulated by the human and the slave-robot follows its motions. This is frequently used for the direct control of a single robot but also in shared control of a cooperative team [LS05]. It is also common for master-slave systems to provide reactive force-feedback to the user, i.e. the force necessary to conduct the commanded motion is reflected to the operator and impacts the human motion. In such a set-up the human hand is modelled as a mechanic impedance [Hog89]. In supervisory architectures the user typically directs the system via a data processing station on a higher level [PST+15]. For shared control many conceivable interfaces exist, e.g. motion capturing [SMH15], hand gesture recognition [GFS+14] or video game controllers (see figure 1.1). The latter are used to control a teleoperated robot inside the Fukushima Daiichi Nuclear Power Station. The robot shown in fig. 1.1a is equipped with two arms to cooperatively manipulate tools.

The aforementioned input methods have in common that the user is not provided with reactive force-feedback. There is no counteracting force or maximum deflection barrier to limit the possible inputs, thus the user may command arbitrary trajectories. Consider a robotic set-up driven into an obstacle and a user persisting to command motion in the blocked direction. Contact forces and desired velocity become an infinite source of energy. Thus it is indispensable to consider commands that may destabilize the system and/or endanger the environment, especially humans on-site.

Concerning safety, a number of collision detection and response strategies exist to make the robot behaviour safe when it comes in contact with a human [Had14]. These methods work well for slow motion, but for fast and sudden impacts the closed-loop bandwidth of the robots is too slow. The robot's dynamics is then dominated by its effective inertia [LTC12]. A general solution is to limit the energy stored in the robotic set-up. In an unexpected collision the exchangeable energy is then bounded [TdVS14]. Empirical studies relate severe injuries of humans to the energetic state of the robot [Woo71, YPM+96].
Towards a conclusion on closed-loop stability of such a set-up, the major challenge is the unknown dynamic behaviour of the human and the non-restrictive input interfaces. Seen from a control point of view, the human decision making is a "black box", the inputs and outputs are available, but the internal behaviour is unknown. Psychological models based on empirical studies and neural network structures [PST+15] emulate human behaviour. However, there is no way to guarantee successful modelling of the unpredictable human behaviour. Thus they do not qualify to be the base of a stability proof of the closed-loop behaviour.
The objective of this thesis is two-fold: first, a shared control architecture for cooperative object manipulation is designed. Applying the leader-follower paradigm, a human commands the object motion, while the robots autonomously maintain the coordination (chapter 2). The controller is passive, i.e. is asymptotically stable with any environment iff the energy supply is finite. Therefore the second goal is an energy shaping approach to cope with an unmodeled human in the loop, who can command arbitrary trajectories and thus supply infinite energy. Bounding the energy in the system ensures closed loop stability and enhances the safety for humans in the environment of the robots (chapter 3).
Energy is a major entity in this thesis, a power-consistent formulation allows insights into energy flow and facilitates stability proofs. Thus it is functional to choose an energy-based system description. The port-Hamiltonian representation additionally allows a model-based controller design.
Chapter 2 starts with a general introduction to the port-Hamiltonian framework and details on the description of 3D-mechanical systems. By interconnection of virtual mechanical elements two model-based controllers are designed.
Chapter 3 introduces an energy tank to limit the energy supply to the controllers designed in chapter 2. An adaptive coupling of user and robots is proposed to shape the energy exchange dependent on the tank level.
Chapter 4 presents simulation results of the schemes developed in chapter 2 and compares them to known approaches. The effectiveness of the energy-bounded trajectory tracking is also verified by simulation.
Chapter 5 draws a brief conclusion and some remarks on future directions are given.

1.1 Problem Statement

Multiple robots manipulate a common object, the human user guides the formation by hand motion. There are two major challenges to be considered in this type of human-robot team interaction: 1) How to address the coordination of the multiple robots in order to let the operator focus on object motion; 2) How to achieve stability and safety with the human in the loop.
The full set-up of human-robot team interaction to analyse and model is shown in figure 1.2. The user does not interact physically with the robots, but is virtually coupled in the manner of a leader-follower scheme. When cooperatively handling an object, the robots need to preserve a certain formation to avoid dropping or excessive squeezing of the object.
Thus the controller has two tasks, 1) to ensure trajectory following with respect to the human motion (high-level task), 2) to generate suitable trajectories for each robot to respect the coordination requirements (low-level task). The control scheme to be designed is thus shared, since it has an autonomous part (formation preservation) and a human command part (movement of the formation).
In such a shared control set-up the control loop encompasses the human and the environment the robot team interacts with. Towards stability and safety the major challenge is the largely unknown dynamics of both human and environment. Input interfaces that do not restrict the human commands, either by a counteracting force, or maximum deflection, allow for infeasible and/or unsafe trajectories. It is the objective of the controller to achieve safe and stable operation for arbitrary inputs.

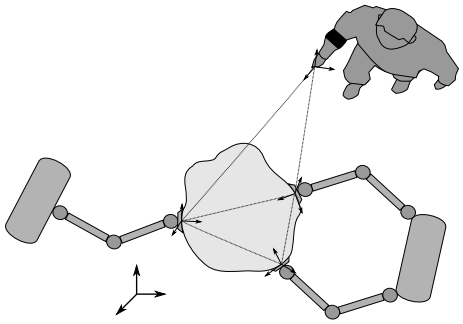

Figure 1.2: A human user interacting with a robotic team cooperatively grasping and manipulating an object

1.2 Cooperative manipulation and energy regulation control

A number of classic control schemes for cooperative object manipulation are object-centred and therefore qualify for shared control approaches. They use the so-called *grasp matrix* to relate object and manipulator motion and force distribution [CM08]. The first to use also the impedance control paradigm [Hog84b] in cooperative manipulation tasks are Schneider and Cannon [SC92]. They establish a compliant relation between the desired and the actual object pose. Bonitz and Hsia [BH96] use an impedance relation between the object and each manipulator. This is essential to ensure stability during contact and non-contact transitions. Both impedance relations are combined in [CV01, CCMV08] and more recent in [HKDN13]. Notably the latter elaborates on (asymptotic) stability of the control scheme with a known environment.
The mentioned control schemes employ second-order impedance control to achieve a very dynamic trajectory tracking but are not passive. The cancellation of open-loop dynamics generates possibly unbounded energy. Stramigioli [Str15] points out the effectiveness of passivity when dealing with unknown environments, as for every non-passive controller a passive environment exists that destabilizes the overall system.
Stability with unknown environments, which can only supply a limited amount of energy, is achieved by the *Intrinsically Passive Controller* [Str01b]. The original version has no dampers in parallel with the springs and thus has a weak dynamic performance. Different implementations on the DLR Hand II [WOH06, WOH08] add the dampers along the springs. Instead of using the grasp matrix to describe the kinematic relations of object and manipulators, a virtual structure with a simulated object is introduced. Virtual structures are a well known tool in *formation control* to establish a certain geometric shape of several robotic manipulators [LBY03]. Virtual springs and dampers are used in [VSvdSP14] to coordinate the formation driving of a group a wheeled robots. The Intrinsically Passive Controller features a virtual structure of springs, dampers and a mass (the virtual pendant of the common object). Asymptotic stability follows from the passive nature of the (virtual) mechanical elements [Str15]. Recently, Sieber et al. [SMH15] establish formation control of several manipulators around a common object and study the control options for a human to direct the closed formation.
A human operator is easily included in the formation by virtual spring coupling, especially when in a leader-follower scheme [SMP14]. The human leader can be virtually connected to all or some robots [SMH15], a certain point (e.g. the geometric center of the formation) [WOH06], or an element of the virtual structure (e.g. the manipulated object) [Str01b].
The concept of passivity is widely used when including a human in the control loop [HB12]. Passive systems either store or dissipate supplied energy, i.e. they reach an energetic equilibrium, iff the energy supply is finite. Thus the only requirement

to achieve stability with a passive robot team is, for the human, to supply only a bounded amount of energy [Str15]. To guarantee that only a certain amount of energy is available, an *energy tank* replaces the human to provide energy to the robots. When combined with a proper re-filling strategy the tank concept effectively limits the rate of energy exchange. Known applications of tanks are variable rate haptics [LH10] and teleoperation over delayed communication lines [FSM+11]. Re-filling is necessary because performing actions on the environment usually consumes energy, i.e. energy is permanently withdrawn from the system.
In addition, a tank sourced system can be controlled dependent on its energetic state. The general concept, of actively stabilizing a system at a certain energy level, is usually called *energy shaping control* [OvdSME99]. The energy stored in a robotic system is also a benchmark for possible injuries when it comes to a collision with a human [Woo71, YPM+96]. Approaches to maintain a safe level in single robots modify the given reference trajectory [LTC09], or adapt the internal behaviour of the robot [TdVS14]. Very recent, energy shaping for safety reasons is proposed for a robotic team, that is physically coupled to the human [GSDLP16].
The methodology of energy regulation for teleoperated robotic teams is largely unexplored in literature. Neither are there safety evaluations for cooperative object manipulation tasks. Safety concerns are appropriate because of the higher moving inertias (and thus kinetic energy) in such a set-up. If a user interface allows arbitrary trajectories to be commanded, some require infinite energy for the execution, then passively controlled robots are not sufficient to conclude stability. To the best of the author's knowledge this problem has not been considered so far.

Chapter 2

port-Hamiltonian modelling in cooperative manipualtion tasks

In this chapter a model of the cooperative manipulation system in the port-Hamiltonian framework is introduced. The formulation describes the dynamic behaviour based on the total energy stored in the system. This chapter shows how energy consistent modelling facilitates control design, allows insights into the flow of energy in the system and provides a ready-made stability proof. The first section 2.1 illustrates the advantages of energy-based modelling in more detail. The general theory of port-Hamiltonian systems is presented in section 2.2. The extension of the port-Hamiltonian modelling to six-dimensional mechanical systems is provided in section 2.3.
The modelling of the cooperative set-up starts from a spring-mass-damper system. This composition is a common part of complex mechanical systems and reproduces a compliant contact, the formulation is derived in section 2.4. The counterpart of a compliant contact, namely the constrained contact is treated in section 2.5. Contact descriptions and mechanical elements are the preliminaries to model a cooperative manipulation set-up. Inspired by the virtual structures to achieve a group behaviour in formation control [LBY03], a model-based controller is designed in the last section 2.6.

2.1 Energy-based modelling and control

Every physical process involves energy and especially energy transfers or transformations. Energy allows for a consistent description across different physical domains. Even within the mechanical domain there are two forms of energy (kinetic, potential). Energetic relations do not only define static relations between physical systems but also the dynamic behaviour, described by the transient exchange of energy [OvdSMM01]. The modelling of a complex physical system can therefore be accomplished by an interconnection of simple subsystems, defined by an energy function. A proper combination of such physical elements achieves a desired dy-

namic behaviour and thereby defines a model-based controller on energetic level. In contrast to this, control is traditionally handled from a signal processing viewpoint. Starting from a reference input, an output signal is generated to reduce some error signal. Control design on the energetic level allows to build a model-based controller in a physically meaningful way. An energetically consistent control scheme visualizes the flow of energy in the system (e.g. energy supplied by an operator and distributed to the robots) and enables *passivity-based control* design. Considering the energy balance of the controlled system and explicitly performing control by shaping the energy is the foundation of passivity based control. Passivity-based control in robotics is appropriate when considering interaction with unknown environments (see also chapter 3 and [Str15]).
Another motivation for control design on energy level is safety in physical human-robot interaction or co-working. The kinetic energy stored in the robotic system is intimately connected with the risk of severe injuries of a human. Assume a human controlling a robotic team and as a result supplying energy to the controller, which distributes the energy to the robots. Because of its formulation on the energy level, the controller is aware of the energetic state of the system and adapts its behaviour to keep the energy bounded (see chapter 3).
For the energy-consistent modelling of mechanical systems two approaches are known: the *Lagrangian* and the *Hamiltonian* approach. Since a combination of the Hamiltonian description and port-based interconnection is developed in recent years, we refer to port-Hamiltonian modelling. It allows to describe complex physical systems based on the interconnection of simpler subsystems, represented in a convenient input-state-output formulation, which has the structure of a (non-linear) state space formulation. The Hamiltonian function of the interconnected system sums up the total energy stored in the subsystem and is a *Lyapunov* candidate function, facilitating stability proofs.

2.2 port-Hamiltonian description of mechanical systems

For the derivation of the port-Hamiltonian description of a mechanical system we start from the classical *Euler-Lagrange* equations of motion

$$\frac{d}{dt}\left(\frac{\partial \mathcal{L}}{\partial \dot{\boldsymbol{q}}}\right) - \frac{\partial \mathcal{L}}{\partial \boldsymbol{q}} = G(\boldsymbol{q})\boldsymbol{u}, \tag{2.1}$$

where $\boldsymbol{q} \in \mathbb{R}^k$ is the vector of generalized configuration coordinates of the system. The *Lagrangian* $\mathcal{L} = V_\mathrm{K} - V_\mathrm{P}$ equals the difference between the kinetic co-energy V_K and the potential energy V_P. The kinetic co-energy is explicitly given as $V_\mathrm{K} = \frac{1}{2}\dot{\boldsymbol{q}}^T M(\boldsymbol{q})\dot{\boldsymbol{q}}$, with a symmetric, positive definite inertia matrix $M(\boldsymbol{q}) \in \mathbb{R}^{k\times k}$. The generalized forces $\boldsymbol{u} \in \mathbb{R}^m$ act on the system with an input matrix $G(\boldsymbol{q}) \in \mathbb{R}^{k\times m}$.

We define the generalized *momenta* for every Lagrangian $\boldsymbol{p} := \frac{\partial \mathcal{L}}{\partial \dot{\boldsymbol{q}}}$ and obtain $\boldsymbol{p} = M(\boldsymbol{q})\dot{\boldsymbol{q}}$. The *Hamiltonian* (energy) function

$$\mathcal{H}(\boldsymbol{q}, \boldsymbol{p}) = \underbrace{\boldsymbol{p}^T \dot{\boldsymbol{q}}}_{2V_\mathrm{K}} - \underbrace{\mathcal{L}(\boldsymbol{q}, \dot{\boldsymbol{q}})}_{V_\mathrm{K} - V_\mathrm{P}} \tag{2.2}$$

allows to rewrite the Euler-Lagrange equation in form of the classical Hamiltonian equations of a mechanical system

$$\begin{aligned} \dot{\boldsymbol{q}} &= \frac{\partial \mathcal{H}}{\partial \boldsymbol{p}}(\boldsymbol{q}, \boldsymbol{p}) \\ \dot{\boldsymbol{p}} &= -\frac{\partial \mathcal{H}}{\partial \boldsymbol{q}}(\boldsymbol{q}, \boldsymbol{p}) + G(\boldsymbol{q})\boldsymbol{u} \end{aligned} \tag{2.3}$$

Equation (2.2) that the Hamiltonian is the sum of kinetic and potential energy, i.e. the total energy stored in the system [vdS06]. The energy balance is

$$\frac{d}{dt}\mathcal{H} = \frac{\partial^T \mathcal{H}}{\partial \boldsymbol{q}}(\boldsymbol{q}, \boldsymbol{p})\dot{\boldsymbol{q}} + \frac{\partial^T \mathcal{H}}{\partial p}(\boldsymbol{q}, \boldsymbol{p})\dot{\boldsymbol{p}} = \boldsymbol{u}^T G^T(\boldsymbol{q})\dot{\boldsymbol{q}} = \boldsymbol{u}^T \boldsymbol{y} \tag{2.4}$$

Hamiltonian systems are energy conservative, i.e. the supplied energy is stored in the system. In equation 2.4 a new output $\boldsymbol{y} = G^T(\boldsymbol{q})\dot{\boldsymbol{q}}$ is introduced. Clearly the product $\boldsymbol{y}^T\boldsymbol{u}$ is the exchanged power and the pair $(\boldsymbol{u}, \boldsymbol{y})$ is called a *power port*. The general equations of a port-Hamiltonian system are

$$\begin{aligned} \dot{\boldsymbol{q}} &= \frac{\partial \mathcal{H}}{\partial \boldsymbol{p}}(\boldsymbol{q}, \boldsymbol{p}) \\ \dot{\boldsymbol{p}} &= -\frac{\partial \mathcal{H}}{\partial \boldsymbol{q}}(\boldsymbol{q}, \boldsymbol{p}) + G(\boldsymbol{q})\boldsymbol{u} \\ \boldsymbol{y} &= G^T(\boldsymbol{q})\frac{\partial \mathcal{H}}{\partial \boldsymbol{p}}(\boldsymbol{q}, \boldsymbol{p}) \end{aligned} \tag{2.5}$$

Port-Hamiltonian systems are suitable to describe a variety of physical systems including mechanical, electrical, thermal and hydraulic elements, see [DMSB09] for an overview. The common ground across the physical domains is the Hamiltonian energy function and inputs and outputs being dual quantities (e.g. velocity-force, current-voltage, heat flow-temperature change). To emphasize this inherent relation, inputs $\boldsymbol{u}$ are called *flows* and outputs $\boldsymbol{y}$ are called *efforts*. A more formal definition of ports, efforts and flows can be found in the next subsection 2.2.1. The general appearance of a port-Hamiltonian system in the form of a (non-linear) state-space formulation becomes apparent in the following example.

Example 2.1:
Consider a simple one-dimensional spring-mass system described by the equation $m\ddot{x} = -kx + F$ and shown in figure 2.1. The parameters m, k, F denote the mass, stiffness and external force acting on the mass respectively. A state space formulation of the system is

$$\begin{pmatrix} \dot{x} \\ \ddot{x} \end{pmatrix} = \begin{pmatrix} 0 & 1 \\ -\frac{k}{m} & 0 \end{pmatrix} \begin{pmatrix} x \\ \dot{x} \end{pmatrix} + \begin{pmatrix} 0 \\ 1 \end{pmatrix} \frac{F}{m} \tag{2.6}$$

In the Hamiltonian approach the system is described based on the energy functions, being $V_{\mathrm{P}}(q) = \frac{1}{2}kq^2$ for the spring and $V_{\mathrm{K}}(p) = \frac{1}{2m}p^2$ for the mass. The total energy is thus the Hamiltonian $\mathcal{H}(q,p) = V_{\mathrm{K}} + V_{\mathrm{P}}$ The state variables are thus replaced by the energy states, the *configuration* $q = x$ accounting for the spring and the *momentum* $p = m\dot{x}$ accounting for the mass.

$$\begin{aligned} \begin{pmatrix} \dot{q} \\ \dot{p} \end{pmatrix} &= \begin{pmatrix} 0 & 1 \\ -1 & 0 \end{pmatrix} \begin{pmatrix} \frac{\partial \mathcal{H}}{\partial q}(q,p) \\ \frac{\partial \mathcal{H}}{\partial p}(q,p) \end{pmatrix} + \begin{pmatrix} 0 \\ 1 \end{pmatrix} F \\ y &= \begin{pmatrix} 0 & 1 \end{pmatrix} \begin{pmatrix} \frac{\partial \mathcal{H}}{\partial q}(q,p) \\ \frac{\partial \mathcal{H}}{\partial p}(q,p) \end{pmatrix} \end{aligned} \tag{2.7}$$

Key aspect of port-Hamiltonian system is the division into atomic energy storing elements (spring, mass) and their proper interconnection. In the example this is done implicitly by defining energy functions and states for both elements. The rules of interconnection are explicitly given by:

- equal velocity of a spring tip and the mass $\dot{x} = \frac{\partial \mathcal{H}}{\partial p}$(rigid connection)
- opposite forces at the spring tip and the mass $\dot{p} = -\frac{\partial \mathcal{H}}{\partial q} + F$ (principle of action-reaction)

Due to the *second law of thermodynamics* real mechanical systems are never energy conservative. Consequently the modelling requires energy dissipating elements (since thermal energy is "lost" w.r.t. the mechanical domain). A mechanical system is then described by its basic elements: springs, masses and dampers. Table 2.1 gives an overview of the elements and their characterizing quantities. Note that dissipation elements do not have a state because they do not store energy.
Next to *energy-storing* and *-dissipating* there is a third class of elements, namely *energy-conservative* structures. Elements within this group are transformers, gyrators and ideal constraints. They are used to redirect the power flow in the system. It is possible to merge all *energy-storing* elements into a single object representation (see Fig. 2.2). Analogously this can be done for the dissipation elements. The interconnecting structure (denoted by $\mathcal{D}$ in Fig. 2.2), consisting of the *energy-conservative* elements, formalizes the energy routing and geometric dependencies of the system. A detailed explanation is given in the next subsection.

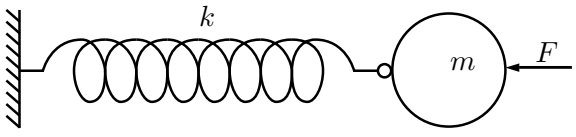

Figure 2.1: Spring-mass example

Table 2.1: port-Hamiltonian system variables of mechanical elements

	Spring	**Mass**	**Damper**
Effort variable	Force F	Velocity $\dot{x}$	Force F
Flow variable	Velocity $\dot{x}$	Force $F = \dot{p}$	Velocity $\dot{x}$
State variable	Position x	Momentum p	-
Energy function	$E(x) = \frac{1}{2}kx^2$	$E(p) = \frac{p^2}{2m}$	$E(\dot{x}) = D\dot{x}^2$ (diss. co-energy)

Complex physical systems can be modelled as a network of energy storing and dissipating elements, for example an electrical network consisting of resistors, inductors and capacitors. The rules of interconnection are Newton's third law (action-reaction), Kirchhoff's laws and power-conserving elements like transformers or gyrators. The aim of port-Hamiltonian modelling is to describe the power-conserving elements with the interconnection laws as a geometric structure and to define the Hamiltonian function as the total energy of the system.
The input-output pair $(\boldsymbol{u}, \boldsymbol{y})$ formalizes the system's external energy exchange. The externally supplied energy is internally either stored or dissipated. The flow of stored and dissipated power is also formalized by a power port respectively. All sub-flows and -efforts in the system are elements of a general set of flows $\boldsymbol{f}$ and efforts $\boldsymbol{e}$. The following subsection 2.2.1 gives formal definitions of the internal and external energy exchange of a port-Hamiltonian system.

2.2.1 Dirac structures and interconnection ports

The energy-routing structure forms the basis of every port-Hamiltonian system. It can be compared to the printed circuit board in electronics, where capacitors, inductors and resistors are the energy-storing and damping elements. Mathematically it has the form of a *Dirac* structure [vdS06]. The main property of a Dirac structure is power conservation, i.e. the power flowing into and out of it always sums to zero. Thus the set of ports $(\boldsymbol{f}, \boldsymbol{e})$ connecting to the Dirac structure $\mathcal{D}$ has the property

$$\boldsymbol{e}^T \boldsymbol{f} = 0 \quad \forall (\boldsymbol{f}, \boldsymbol{e}) \in \mathcal{D} \tag{2.8}$$

where $\mathcal{D}$ is a subspace of the space of flow and effort $\mathcal{D} \subset \mathcal{E} \times \mathcal{F}$. The space of flows is $\boldsymbol{f} \in \mathcal{F}$, the space of efforts is its dual linear space $\boldsymbol{e} \in \mathcal{E} = \mathcal{F}^*$. The Dirac

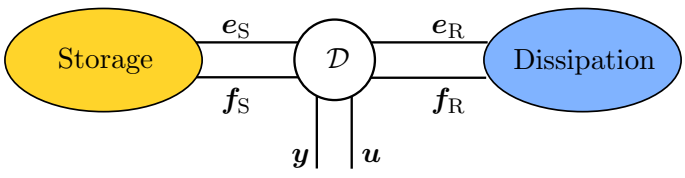

Figure 2.2: port-Hamiltonian system structure

structure has the same dimension as the space of flows $dim\mathcal{D} = dim\mathcal{F}$. Further mathematical requirements can be found in literature [vdS06, vdSJ14].
Power conservation means that supplied energy is either stored or dissipated in the system. All storing and resistive elements can be grouped as shown in figure 2.2. Three ports join in the interconnection structure, one for the external supply $(\boldsymbol{u}, \boldsymbol{y})$, one for the sum of storing elements $(\boldsymbol{f}_\mathrm{S}, \boldsymbol{e}_\mathrm{S})$ and one for the resistive elements $(\boldsymbol{f}_R, \boldsymbol{e}_R)$. Mathematically the interconnection of ports is defined by the Dirac structure matrix $S_\mathcal{D}$

$$\begin{pmatrix} \boldsymbol{y} \\ \boldsymbol{f}_\mathrm{S} \\ \boldsymbol{e}_\mathrm{R} \end{pmatrix} = S_\mathcal{D} \begin{pmatrix} \boldsymbol{u} \\ \boldsymbol{e}_\mathrm{S} \\ \boldsymbol{f}_\mathrm{R} \end{pmatrix} \tag{2.9}$$

It can be shown that for a skew-symmetric $S_\mathcal{D}$ the power balance of the ports is

$$\boldsymbol{e}_\mathrm{S}{}^T \boldsymbol{f}_\mathrm{S} + \boldsymbol{y}^T \boldsymbol{u} + \boldsymbol{e}_\mathrm{R}{}^T \boldsymbol{f}_\mathrm{R} = 0, \tag{2.10}$$

which fulfils the desired power conservation.
A further simplification of equation 2.3 is achieved by setting $\boldsymbol{x} = (\boldsymbol{q}^T, \boldsymbol{p}^T)^T$. One obtains a generalization to the standard state-space representation

$$\begin{aligned} \dot{\boldsymbol{x}} &= [J(\boldsymbol{x}) - D(\boldsymbol{x})] \frac{\partial \mathcal{H}}{\partial \boldsymbol{x}}(\boldsymbol{x}) + G(\boldsymbol{x})\boldsymbol{u} \\ \boldsymbol{y} &= G^T(\boldsymbol{x}) \frac{\partial \mathcal{H}}{\partial \boldsymbol{x}}(\boldsymbol{x}), \end{aligned} \tag{2.11}$$

with $J(\boldsymbol{x}) \in \mathbb{R}^{2k \times 2k}$ being a skew-symmetric structure matrix and $D(\boldsymbol{x}) \in \mathbb{R}^{2k \times 2k}$ being a positive semi-definite, symmetric dissipation matrix.
Each power port, as shown in 2.2, contributes to the energy balance of the system and influences the dynamic behaviour. The external port is used to interconnect two port-Hamiltonian systems.

Energy storage port

The energy storage port accounts for the internal storage of the system, its port variables are $(\boldsymbol{f}_\mathrm{S}, \boldsymbol{e}_\mathrm{S})$. The power supplied through this port is stored in the Hamiltonian energy function $\mathcal{H}(\boldsymbol{x})$ of the system. The resulting energy balance is:

$$\frac{d}{dt}\mathcal{H} = \frac{\partial^T \mathcal{H}}{\partial \boldsymbol{x}}(\boldsymbol{x})\dot{\boldsymbol{x}} \tag{2.12}$$

The flow variable is the energy rate $\boldsymbol{f}_\mathrm{S} = -\dot{\boldsymbol{x}}$ and the effort variable is $\boldsymbol{e}_\mathrm{S} = \frac{\partial \mathcal{H}}{\partial \boldsymbol{x}}(\boldsymbol{x})$.

Energy dissipation port

The energy dissipation port corresponds to internal dissipation and can be used to model resistive elements. The port variables are described by the general resistive relation

$$F(\boldsymbol{f}_\mathrm{R}, \boldsymbol{e}_\mathrm{R}) = 0 \tag{2.13}$$

with the property ${\boldsymbol{e}_{\mathrm{R}}}^T \boldsymbol{f}_{\mathrm{R}} \leq 0$ (energy dissipation). An important special case is the input-output resistive relation $\boldsymbol{f}_{\mathrm{R}} = -F(\boldsymbol{e}_{\mathrm{R}})$. For linear elements simply

$$\boldsymbol{f}_{\mathrm{R}} = -R\boldsymbol{e}_{\mathrm{R}} \ , \ R = R^T \succeq 0 \tag{2.14}$$

For an uncontrolled system that does not interact with the environment, i.e. there is no energy exchange through the external port, the energy balance is:

$$\frac{d\mathcal{H}}{dt} = -{\boldsymbol{e}_{\mathrm{S}}}^T \boldsymbol{f}_{\mathrm{S}} = {\boldsymbol{e}_{\mathrm{R}}}^T \boldsymbol{f}_{\mathrm{R}} \leq 0 \tag{2.15}$$

External port

The external port $(\boldsymbol{u}, \boldsymbol{y})$ can be further split into an environment *interaction* $(\boldsymbol{f}_{\mathrm{I}}, \boldsymbol{e}_{\mathrm{I}})$ and a *control* port $(\boldsymbol{f}_{\mathrm{C}}, \boldsymbol{e}_{\mathrm{C}})$, satisfying $\boldsymbol{y}^T\boldsymbol{u} = {\boldsymbol{e}_{\mathrm{I}}}^T \boldsymbol{f}_{\mathrm{I}} + {\boldsymbol{e}_{\mathrm{C}}}^T \boldsymbol{f}_{\mathrm{C}}$. The power balance of the whole system then is

$${\boldsymbol{e}_{\mathrm{S}}}^T \boldsymbol{f}_{\mathrm{S}} + {\boldsymbol{e}_{\mathrm{R}}}^T \boldsymbol{f}_{\mathrm{R}} + {\boldsymbol{e}_{\mathrm{I}}}^T \boldsymbol{f}_{\mathrm{I}} + {\boldsymbol{e}_{\mathrm{C}}}^T \boldsymbol{f}_{\mathrm{C}} = 0 \tag{2.16}$$

or by using (2.12)

$$\frac{d\mathcal{H}}{dt} = {\boldsymbol{e}_{\mathrm{R}}}^T \boldsymbol{f}_{\mathrm{R}} + {\boldsymbol{e}_{\mathrm{I}}}^T \boldsymbol{f}_{\mathrm{I}} + {\boldsymbol{e}_{\mathrm{C}}}^T \boldsymbol{f}_{\mathrm{C}} \tag{2.17}$$

2.2.2 Interconnection of port-Hamiltonian systems

It is important to notice that the interconnection of two port-Hamiltonian systems is again a port-Hamiltonian system [vdSJ14]. Consider two general systems $(i = 1, 2)$ with yet unconnected control and environment interaction ports:

$$\begin{aligned} \dot{\boldsymbol{x}}_i &= [J_i - R_i] \frac{\partial \mathcal{H}_i}{\partial \boldsymbol{x}_i} + \begin{pmatrix} G_{\mathrm{C},i} & G_{\mathrm{I},i} \end{pmatrix} \begin{pmatrix} \boldsymbol{f}_{\mathrm{C},i} \\ \boldsymbol{f}_{\mathrm{I},i} \end{pmatrix} \\ \begin{pmatrix} \boldsymbol{e}_{\mathrm{C},i} \\ \boldsymbol{e}_{\mathrm{I},i} \end{pmatrix} &= \begin{pmatrix} G_{\mathrm{C},i}^T \\ G_{\mathrm{I},i}^T \end{pmatrix} \frac{\partial \mathcal{H}_i}{\partial \boldsymbol{x}_i} \end{aligned} \tag{2.18}$$

where J_i, R_i are a skew-symmetric structure matrix and a positive semi-definite symmetric dissipation matrix, respectively. The input matrices $G_{\mathrm{C},i}$, $G_{\mathrm{I},i}$ describe the effect of a control action and the environment interaction respectively. For notational convenience the usual dependencies on the states are omitted.
The control inputs and outputs are now connected by setting $\boldsymbol{f}_{\mathrm{C},1} = \boldsymbol{e}_{\mathrm{C},2}$ and $\boldsymbol{f}_{\mathrm{C},2} = -\boldsymbol{e}_{\mathrm{C},1}$. Note that the minus sign is necessary for power conservation. The power exchanged by the i-th system is $P_i = {\boldsymbol{e}_{\mathrm{C},i}}^T \boldsymbol{f}_{\mathrm{C},i}$, therefore the total exchanged energy fulfils $P_1 + P_2 = 0$. The resulting interconnected system still has the environment interaction ports open:

$$\begin{aligned} \dot{\boldsymbol{x}} &= [J - R] \frac{\partial \mathcal{H}}{\partial \boldsymbol{x}} + \begin{pmatrix} G_{\mathrm{I},1} & G_{\mathrm{I},2} \end{pmatrix} \begin{pmatrix} \boldsymbol{f}_{\mathrm{I},1} \\ \boldsymbol{f}_{\mathrm{I},2} \end{pmatrix} \\ \begin{pmatrix} \boldsymbol{e}_{\mathrm{I},1} \\ \boldsymbol{e}_{\mathrm{I},2} \end{pmatrix} &= \begin{pmatrix} G_{\mathrm{I},1}^T \\ G_{\mathrm{I},2}^T \end{pmatrix} \frac{\partial \mathcal{H}}{\partial \boldsymbol{x}} \end{aligned} \tag{2.19}$$

where $\boldsymbol{x} = (\boldsymbol{x}_1^T, \boldsymbol{x}_2^T)^T$ and $\mathcal{H} = \mathcal{H}_1 + \mathcal{H}_2$ is the sum of the two energies. The structure and dissipation matrix become:

$$J = \begin{pmatrix} J_1 & G_{\mathrm{C},1} G_{\mathrm{C},2}^T \\ -G_{\mathrm{C},2} G_{\mathrm{C},1}^T & J_2 \end{pmatrix}, \; D = \begin{pmatrix} D_1 & 0 \\ 0 & D_2 \end{pmatrix}$$

2.2.3 port-Hamiltonian systems and passivity

A system is *passive* [OvdSMM01], if there exists a differentiable storage function $\mathcal{H}(\boldsymbol{x}) \geq 0$ that satisfies

$$\frac{d}{dt}\mathcal{H}(\boldsymbol{x}(t)) \leq \boldsymbol{u}^T(t)\boldsymbol{y}(t) \tag{2.20}$$

The product of the input-output pair $(\boldsymbol{u}, \boldsymbol{y})$ is the supplied power. By definition the Hamiltonian function represents the total energy stored in the system. For a port-Hamiltonian system of the form of equation (2.11) the energy balance is

$$\begin{aligned} \frac{d}{dt}\mathcal{H}(\boldsymbol{x}) &= \frac{\partial^T \mathcal{H}}{\partial \boldsymbol{x}} \frac{d\boldsymbol{x}}{dt} = \frac{\partial^T \mathcal{H}}{\partial \boldsymbol{x}} \left[(J(\boldsymbol{x}) - D(\boldsymbol{x})) \frac{\partial \mathcal{H}}{\partial \boldsymbol{x}} + G(\boldsymbol{x})\boldsymbol{u} \right] \\ &= \frac{\partial^T \mathcal{H}}{\partial \boldsymbol{x}} J(\boldsymbol{x}) \frac{\partial \mathcal{H}}{\partial \boldsymbol{x}} - \frac{\partial^T \mathcal{H}}{\partial \boldsymbol{x}} D(\boldsymbol{x}) \frac{\partial \mathcal{H}}{\partial \boldsymbol{x}} + (G^{-T}(\boldsymbol{x})e)^T G(\boldsymbol{x})\boldsymbol{u} \\ &= \boldsymbol{y}^T \boldsymbol{u} - \frac{\partial^T \mathcal{H}}{\partial \boldsymbol{x}} D(\boldsymbol{x}) \frac{\partial \mathcal{H}}{\partial \boldsymbol{x}} \end{aligned} \tag{2.21}$$

The property $\frac{\partial^T \mathcal{H}}{\partial \boldsymbol{x}} J(\boldsymbol{x}) \frac{\partial \mathcal{H}}{\partial \boldsymbol{x}} = 0$ holds for a skew symmetric matrix $J(\boldsymbol{x}) = -J(\boldsymbol{x})^T$. The product of the input-output pair $\boldsymbol{y}^T\boldsymbol{u}$ is the power supplied to the system. Since $D(\boldsymbol{x}) = D(\boldsymbol{x})^T \succeq 0$ is symmetric and positive semi-definite, it is $\frac{\partial^T \mathcal{H}}{\partial \boldsymbol{x}} D(\boldsymbol{x}) \frac{\partial \mathcal{H}}{\partial \boldsymbol{x}} \geq 0$. Conclusively every port-Hamiltonian system, that satisfies the properties equation (2.11), is passive in the sense of equation 2.20. If $R = 0$, i.e. the system exhibits no dissipation and is termed as *lossless*. Passivity is a sufficient criterion for asymptotic stability [OvdSMM01].

2.3 3D-space modelling of mechanical systems

2.3.1 Euclidean space and motions

Coordinate frames

A coordinate frame of the three-dimensional Euclidean space is a 4-tuple of the form $\Psi = (\boldsymbol{o}, \hat{\boldsymbol{x}}, \hat{\boldsymbol{y}}, \hat{\boldsymbol{z}})$, where $\boldsymbol{o}$ is the three-dimensional vector of the origin and $\hat{\boldsymbol{x}}, \hat{\boldsymbol{y}}, \hat{\boldsymbol{z}}$ are the linear independent, orthonormal coordinate vectors. Consider two coordinate frames Ψ_1, Ψ_2 which share the same origin but differ in orientation due to different choices of $\hat{\boldsymbol{x}}_i, \hat{\boldsymbol{y}}_i, \hat{\boldsymbol{z}}_i, \; i = 1, 2$. The change of orientation from Ψ_i to Ψ_j is described

by the rotation matrix R_i^j. The set of rotation matrices is called *special orthonormal* group ($SO(3)$) [Str01a] and is defined as:

$$SO(3) = \{\mathrm{R} \in \mathbb{R}^{3\times 3} \mid \mathrm{R}^{-1} = \mathrm{R}^T, \mathrm{detR} = 1\} \tag{2.22}$$

Sometimes it is useful to define non-inertial frames, e.g. attached to a rigid body. Generally these frames do not share the origin with a the inertial frame. Consider two frames Ψ_i, Ψ_j with different origins then $\boldsymbol{p}_i^j = \boldsymbol{o}_j - \boldsymbol{o}_i$ denotes the distance between the origins. In general, a change between coordinate frames, which differ in position and orientation is expressed with the homogenous matrix

$$H_i^j := \begin{pmatrix} \mathrm{R}_i^j & \boldsymbol{p}_i^j \\ \mathbf{0}_{1\times 3} & 1 \end{pmatrix} \tag{2.23}$$

A point $\boldsymbol{p}^i \in \mathbb{R}^3$ expressed in Ψ_i is cast into Ψ_j by

$$\begin{pmatrix} \boldsymbol{p}^j \\ 1 \end{pmatrix} = H_i^j \begin{pmatrix} \boldsymbol{p}^i \\ 1 \end{pmatrix} \tag{2.24}$$

. The inverse transformation H_j^i is given by

$$H_i^j = (H_i^j)^{-1} = \begin{pmatrix} (\mathrm{R}_i^j)^T & -(\mathrm{R}_i^j)^T \boldsymbol{p}_i^j \\ \mathbf{0}_{1\times 3} & 1 \end{pmatrix} \tag{2.25}$$

and is still a homogeneous matrix. The set of homogeneous matrices is called the *special Euclidean* group:

$$SE(3) := \{ \begin{pmatrix} \mathrm{R} & \boldsymbol{p} \\ \mathbf{0} & 1 \end{pmatrix} \mid \mathrm{R} \in SO(3), \boldsymbol{p} \in \mathbb{R}^3 \} \tag{2.26}$$

The $SE(3)$ is a matrix Lie group, composed of the set of homogeneous matrices H_i^j and the matrix multiplication being the group operation. For more information on Lie groups see e.g. [Str01b].

Twists and wrenches

Consider any point $\boldsymbol{p}^i$ not moving in the coordinate frame Ψ_i, i.e. $\dot{\boldsymbol{p}}^i = 0$. If $\boldsymbol{p}$ is moving in another coordinate frame Ψ_j, the two frames move with respect to each other. The trajectory can be described as a function of time: $H_i^j(t) \in SE(3)$. By differentiating (2.24) one obtains

$$\begin{pmatrix} \dot{\boldsymbol{p}}^j(t) \\ 0 \end{pmatrix} = \dot{H}_i^j(t) \begin{pmatrix} \boldsymbol{p}^i \\ 1 \end{pmatrix}$$

$\dot{H}_i^j$ describes both motion and a change of the reference frame. A representation, that separates $\dot{H}_i^j$ into a homogeneous matrix H_i^j and a velocity variable (twist) $\tilde{T}_i^{j,j}$, is

$$\begin{pmatrix} \dot{\boldsymbol{p}}^j(t) \\ 0 \end{pmatrix} = \tilde{T}_i^{j,j} \left(H_i^j \begin{pmatrix} \boldsymbol{p}^i \\ 1 \end{pmatrix} \right) \tag{2.27}$$

$\dot{H}_i^j$ is a tangential vector along the trajectory $H_i^j(t)$ and thus in the tangent space of the $SE(3)$: $\dot{H}_i^j \in T_{H_i^j}SE(3)$. To obtain a representation of motion which is referenced to a coordinate frame, one can map $\dot{H}_i^j$ to the identity of the $SE(3)$. At the identity e of the $SE(3)$ the tangent space $T_eSE(3)$ has the structure of a Lie algebra. The Lie algebra of the $SE(3)$ is denoted by $\mathfrak{se}(3)$. This is done either by left or right translation, for a definition see [Str01b]. The right translation is used in (2.27) and is written compactly

$$\dot{H}_i^j = \tilde{T}_i^{j,j} H_i^j \tag{2.28}$$

The left translation leads to

$$\dot{H}_i^j = H_i^j \tilde{T}_i^{i,j} \tag{2.29}$$

Left and right translations lead to different representations of a twist:

- $T_i^{k,j}$ is the twist of Ψ_i with respect to Ψ_j expressed in the frame Ψ_k
- $T_i^j = T_i^{j,j}$ is the twist of Ψ_i with respect to Ψ_j expressed naturally in Ψ_j

We call $\tilde{T} \in T_eSE(3)$ a twist and the $\mathfrak{se}(3)$ the space of twists.
To understand the formalism of a twist to describe motion, the derivation from the elements of a homogeneous matrix allows to identify its components

$$\begin{aligned} \tilde{T}_i^j = \dot{H}_i^j H_j^i &= \begin{pmatrix} \dot{\mathrm{R}}_i^j & \dot{\boldsymbol{p}}_i^j \\ \mathbf{0} & 0 \end{pmatrix} \begin{pmatrix} \mathrm{R}_j^i & \boldsymbol{p}_j^i \\ \mathbf{0} & 1 \end{pmatrix} = \begin{pmatrix} \dot{\mathrm{R}}_i^j & \dot{\boldsymbol{p}}_i^j \\ \mathbf{0} & 0 \end{pmatrix} \begin{pmatrix} \mathrm{R}_i^{jT} & -\mathrm{R}_i^{jT} \boldsymbol{p}_i^j \\ \mathbf{0} & 1 \end{pmatrix} \\ &= \begin{pmatrix} \dot{\mathrm{R}}_i^j \mathrm{R}_i^{jT} & -\dot{\mathrm{R}}_i^j \mathrm{R}_i^{jT} \boldsymbol{p}_i^j + \dot{\boldsymbol{p}}_i^j \\ \mathbf{0} & 0 \end{pmatrix} =: \begin{pmatrix} \tilde{\omega}_i^j & \boldsymbol{v}_i^j \\ \mathbf{0} & 0 \end{pmatrix} \end{aligned} \tag{2.30}$$

It is clear from this equation that the linear velocity part $\boldsymbol{v}_i^j$ is not the velocity of the frame Ψ_i with respect to Ψ_j, identified by $\dot{\boldsymbol{p}}_i^j$. This twist representation is described by the *screw theory* (see e.g. [WS08]). It can be visualized by the angular velocity around an axis and the linear velocity along this axis.
Next to the 4×4 matrix $\tilde{T}$ there exists also a vector representation $T \in \mathbb{R}^6$

$$\tilde{T} = \begin{pmatrix} \tilde{\omega} & \boldsymbol{v} \\ \mathbf{0} & 0 \end{pmatrix} \ , \ T = \begin{pmatrix} \boldsymbol{\omega} \\ \boldsymbol{v} \end{pmatrix} \tag{2.31}$$

wherein $\boldsymbol{v} \in \mathbb{R}^3$ is the linear velocity and $\boldsymbol{\omega} \in \mathbb{R}^3$ is the angular velocity. $\tilde{\omega} \in \mathbb{R}^{3\times3}$ is the skew-symmetric representation of the vector $\boldsymbol{\omega}$

$$\boldsymbol{\omega} = \begin{pmatrix} \omega_1 \\ \omega_2 \\ \omega_3 \end{pmatrix} \ \Rightarrow \ \tilde{\omega} = \begin{pmatrix} 0 & -\omega_3 & \omega_2 \\ \omega_3 & 0 & \omega_1 \\ -\omega_2 & \omega_1 & 0 \end{pmatrix} \tag{2.32}$$

Throughout this thesis, vectors assigned with a tilde operator $\tilde{\bullet}$ denote the matrix representation of the vector. This is the matrix crossproduct for a vector of dimension $\mathbb{R}^3$, or the 4×4 representation for a $\mathbb{R}^6$ vector.
Changes of coordinates for twists are of the form

$$\tilde{T}_i^{j,j} = \tilde{T}_i^j = H_i^j \tilde{T}_i^{i,j} H_j^i \tag{2.33}$$

or for the vector representation

$$T_i^j = Ad_{H_i^j} T_i^{i,j} \ , \ Ad_{H_i^j} = \begin{pmatrix} R_i^j & 0 \\ \tilde{p}_i^j R_i^j & R_i^j \end{pmatrix} \tag{2.34}$$

The dual vector space of $\mathfrak{se}(3)$ is the space of linear operations from $\mathfrak{se}(3)$ to $\mathbb{R}$. It is denoted by $\mathfrak{se}^*(3)$ and represents the space of wrenches W. Wrenches decompose to moments $\mathbf{m} \in \mathbb{R}^3$ and forces $\mathbf{f} \in \mathbb{R}^3$.

$$W = (\mathbf{m} \ \ \mathbf{f}) \ , \ \tilde{W} = \begin{pmatrix} \tilde{\mathrm{m}} & \mathbf{f} \\ \mathbf{0} & 0 \end{pmatrix} \tag{2.35}$$

Again $\tilde{W} \in \mathbb{R}^{4\times4}$ is a matrix while $W \in \mathbb{R}^6$ is the row vector representation. The change of coordinates for wrenches is similar to the case of twists:

$$(W_i^{k,i})^T = Ad_{H_k^i}^T (W_i^{i,i})^T \tag{2.36}$$

Here the mapping is in the opposite direction, from Ψ_j to Ψ_i, which is a consequence of the fact that wrenches are duals to twists. Again there are different representations of wrenches:

- $W_i^{k,j}$ is the wrench applied to a spring connecting Ψ_i to Ψ_j on the side of Ψ_i expressed in the coordinate frame Ψ_k.

- W_i^k is the wrench applied to a body attached to Ψ_i expressed in the coordinate frame Ψ_k.

These definitions lead to the following rules of interconnection: connecting a mass and spring in the point Ψ_i and applying the principle of action and reaction one gets $W_i^{k,j} = -W_i^k$. The wrenches on either side of a spring are antisymmetric $W_i^{k,j} = -W_j^{k,i}$
The duality product of flow and effort defines the power flowing through a port, in the mechanical domain this corresponds to the twist and the wrench. On a vector space level the power port $\mathcal{P}$ is defined by the Cartesian product of the Lie algebra $\mathfrak{se}(3)$ and its dual $\mathfrak{se}^*(3)$: $\mathcal{P} = \mathfrak{se}(3) \times \mathfrak{se}^*(3)$.

2.3.2 Input-state-output port-Hamiltonian systems in 3D space

The port-Hamiltonian systems considered so far define the relation of the time-derivative of the configuration $\boldsymbol{q}$ and the change of kinetic energy

$$\frac{\partial \mathcal{H}}{\partial \boldsymbol{p}} = M^{-1}\boldsymbol{p} = \dot{\boldsymbol{q}} \tag{2.37}$$

For six DoF configuration and twist are related by $\dot{H}_i^j = \tilde{T}_i^{j,j} H_i^j$ (eq. 2.3.1). The next section introduces the 3D-description of a mass in the port-Hamiltonian framework, the kinetic (co-)energy function is $\mathcal{H}_\mathrm{K} = \frac{1}{2} {P_i^i}^T M^{-1} P_i^i$, with the momentum $P_i^i = MT_i^{i,0}$. Thus the relation of configuration- and kinetic energy change for six DoF is

$$\frac{\partial \mathcal{H}}{\partial P_i^i} = M^{-1} P_i^i = H_0^i \dot{H}_i^0 \tag{2.38}$$

Consequently the interconnecting Dirac structure depends on the configuration H_0^i and is termed a *modulated* Dirac structure. Mathematically the state space of the system is then a *manifold*, for details see [vdSJ14]. This state manifold $\mathcal{X}$ includes the local coordinates $\boldsymbol{x} \in \mathcal{X}$. The flows towards the energy storage is assigned with $\boldsymbol{f}_\mathrm{S} = -\dot{\boldsymbol{x}}$ and the efforts with $\boldsymbol{e}_\mathrm{S} = \frac{\partial \mathcal{H}}{\partial \boldsymbol{x}}$. The flows are elements of the tangent space $T_x\mathcal{X}$ of the state manifold at the state $\boldsymbol{x} \in \mathcal{X}$ and the efforts are elements of the co-tangent space $T_x^*\mathcal{X}$. The resulting port-Hamiltonian system in 3D space is of the form

$$\begin{aligned} \dot{\boldsymbol{x}} &= [J(\boldsymbol{x}) - D(\boldsymbol{x})] \frac{\partial \mathcal{H}}{\partial \boldsymbol{x}}(\boldsymbol{x}) + G(\boldsymbol{x})\boldsymbol{u} \\ \boldsymbol{y} &= G^T(\boldsymbol{x}) \frac{\partial \mathcal{H}}{\partial \boldsymbol{x}}(x) \end{aligned} \tag{2.39}$$

with a skew-symmetric matrix $J(\boldsymbol{x})$ and a resistive structure matrix $D(\boldsymbol{x})$ which is symmetric and positive semi-definite. Clearly $\boldsymbol{u}$ and $\boldsymbol{y}$ denote the input and output respectively and this representation is again of the *input-state-output* form. In the following section introduces the corresponding representations of atomic mechanical elements.

2.3.3 Modelling of atomic mechanical elements

Springs

A *spring* is the ideal, lossless element storing potential energy. It is connected to two bodies and is defined by a potential energy function. The energy is a function of the relative displacement of the attached bodies. Consider a spring between the two bodies B_i and B_j, with coordinate frames Ψ_i and Ψ_j fixed to the respective bodies. The stored potential energy is positive definite function of the form

$$V_\mathrm{P} : SE(3) \to \mathbb{R};\ H_i^j \mapsto V_\mathrm{P}(H_i^j) \tag{2.40}$$

For explicit energy functions for different types of springs see [Str01b]. The input-state-output form is defined by the relative displacement H_i^j (state variable), the wrench $W_i^{j,j}$ (output) and the twist T_i^j (input).

$$\begin{aligned} \dot{H}_i^j &= T_i^j H_i^j \\ W_i^{j,j} &= \frac{\partial V_{\mathrm{P}}(H_i^j)}{\partial H_i^j}(H_i^j)^T \end{aligned} \tag{2.41}$$

Note that V_{P} is an energetic minimum when H_i^j is the identity matrix I_4. An energetic minimum is physically necessary, otherwise infinite energy would be extractable from the spring. With $H_i^j = I_4$ the frames Ψ_i and Ψ_j coincide. It is possible to define springs with non-zero rest-length by introducing coordinate frames Ψ_{ic} and Ψ_{jc} rigidly attached to Ψ_i and Ψ_j respectively. The spring is now between the new frames, thus the energetic minimum is $H_{ic}^{jc} = I_4$. The displacements H_i^{ic}, H_j^{jc} are the resulting rest-lengths. Frames Ψ_{ic} and Ψ_{jc} can be chosen to represent the *center of stiffness*, where translation and rotation are maximally decoupled [SMA99].

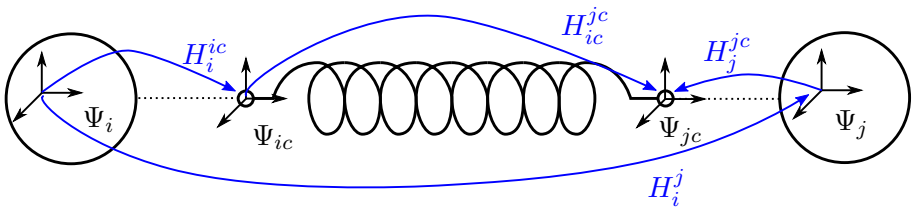

Figure 2.3: Frames and configurations for a variable-restlength spring

Inertias

Inertias are special since they in general store two types of energy: kinetic and potential energy due to gravitation. For simplicity the gravitational terms are excluded at first to allow focus on motion. Kinetic energy is a function of the relative motion w.r.t. an inertial reference. When expressing motion in non-inertial or accelerated reference frames, fictitious forces such as the *Coriolis* or the *centrifugal* force need to be considered.
The derivation of the port-Hamiltonian formulation starts from *Newton's* second law of dynamics. The time derivative of a body's momentum is equal to the applied wrench.

$$\dot{P}_b^0 = W_b^0 \tag{2.42}$$

The momentum of the inertia b and the wrench acting on it are both expressed in the inertial reference frame Ψ_0. Consider the non-inertial frame Ψ_b, assigned to the centre of mass of inertia b. For a change of coordinates to Ψ_b one obtains $W_b^0 = Ad_{H_0^b}^T W_b^b$. It is detailed in [Str01b] that $P_0^b \in \mathfrak{se}^*(3)$ and thus the same transformation

as for wrenches applies $P_b^0 = Ad_{H_0^b}^T P_b^b$. *Newton's* second law is expressed in the non-inertial frame Ψ_b

$$\frac{d}{dt}(Ad_{H_0^b}^T P_b^b) = Ad_{H_0^b}^T W_b^b \tag{2.43}$$

The evolution of the accelerated body frame Ψ_b w.r.t to the inertial frame is time dependent. The time derivative of the transformation is $\frac{d}{dt}Ad_{H_0^b}^T = -Ad_{H_0^b}^T ad_{T_b^{b,0}}^T$, with the *adjoint* representation (see for example [Str01a]):

$$ad_{T_b^{b,0}}^T = \begin{pmatrix} -\tilde{\omega}_b^{b,0} & -\tilde{v}_b^{b,0} \\ 0 & -\tilde{\omega}_b^{b,0} \end{pmatrix} \tag{2.44}$$

The second law of dynamics expressed in the body's frame is then

$$\begin{aligned} Ad_{H_0^b}^T \dot{P}_b^b - Ad_{H_0^b}^T ad_{T_b^{b,0}}^T P_b^b &= Ad_{H_0^b}^T W_b^b \\ \dot{P}_b^b &= ad_{T_b^{b,0}}^T P_b^b + W_b^b \end{aligned} \tag{2.45}$$

This formulation is split into its rotational and translational components, this allows to exchange twist and momentum by the following operation

$$\begin{pmatrix} \dot{P}_{b,\omega}^b \\ \dot{P}_{b,v}^b \end{pmatrix} = \begin{pmatrix} -\tilde{\omega}_b^{b,0} & -\tilde{v}_b^{b,0} \\ 0 & -\tilde{\omega}_b^{b,0} \end{pmatrix} \begin{pmatrix} P_{b,\omega}^b \\ P_{b,v}^b \end{pmatrix} + W_b^b = \begin{pmatrix} \tilde{P}_{b,\omega}^b & \tilde{P}_{b,v}^b \\ \tilde{P}_{b,v}^b & 0 \end{pmatrix} \begin{pmatrix} \omega_b^{b,0} \\ v_b^{b,0} \end{pmatrix} + W_b^b \tag{2.46}$$

This clearly corresponds to the classical description of a rigid body's dynamics of the form

$$\dot{P}_b^b = M_b \dot{T}_b^{b,0} = C_b T_b^{b,0} + W_b^b \tag{2.47}$$

Here M_b describes the body's inertia and C_b accounts for Coriolis and centrifugal terms.

The derivation of a port-Hamiltonian representation starts from the kinetic (co-)energy given by $V_{\mathrm{K}}^*(T_b^{b,0}) = \frac{1}{2}(T_b^{b,0})^T M_b T_b^{b,0}$. Formally speaking the kinetic energy is a function of the momentum. By using the relation of twist and momentum $P_b^b = M_b T_b^{b,0}$, the kinetic energy is

$$V_{\mathrm{K}}(P_b^b) = \frac{1}{2}(P_b^b)^T M_b^{-1} P_b^b \tag{2.48}$$

By differentiating the kinetic energy w.r.t to the state variable P_b^b one obtains

$$\frac{\partial V_{\mathrm{K}}(P_b^b)}{\partial P_b^b} = M_b^{-1} P_b^b = T_b^{b,0} \tag{2.49}$$

Recall from Table 2.1 that the twist is the effort variable in the port-Hamiltonian representation of an inertia. The flow is the externally supplied wrench W_b^b, thus we obtain the port-Hamiltonian representation of a rigid body, neglecting gravity

$$\begin{aligned} \dot{P}_b^b &= C_b \frac{\partial V_{\mathrm{K}}(P_b^b)}{\partial P_b^b} + I_6 W_b^b \\ T_b^{b,0} &= I_6 \frac{\partial V_{\mathrm{K}}(P_b^b)}{\partial P_b^b} \end{aligned} \tag{2.50}$$

The handling of heavy objects is a common use case of cooperative manipulation. It is thus inevitable to include the potential energy resulting from the gravitational field. One can think of a spring connecting the body and an inertial frame associated with the ground. This spring can be formulated in port-Hamiltonian structure using the left translation (2.3.1)

$$\begin{aligned} \dot{H}_b^0 &= H_b^0 T_b^{b,0} \\ W_b^{b,0} &= (H_b^0)^T \frac{\partial V_\mathrm{P}(H_b^0)}{\partial H_b^0}, \end{aligned} \tag{2.51}$$

where V_P is a suitable energy function. For a combined description the potential and kinetic energy add up and the Hamiltonian becomes $\mathcal{H}(P_b^b, H_b^0) = V_\mathrm{K}(P_b^b) + V_\mathrm{P}(H_b^0)$. Since there are two types of energy stored by *one* body, the twists in both energy systems are equal. The wrenches on the body add up

$$W_\Sigma^b = W_b^b + C_b \frac{\partial \mathcal{H}(P_b^b, H_b^0)}{\partial P_b^b} - (H_b^0)^T \frac{\partial \mathcal{H}(P_b^b, H_b^0)}{\partial H_b^0} \tag{2.52}$$

The negative sign on the right hand side of eq. (2.52) is due to the principle of action and reaction.
With this knowledge the combined port-Hamiltonian representation can be written

$$\begin{aligned} \begin{pmatrix} \dot{H}_b^0 \\ \dot{P}_b^b \end{pmatrix} &= \begin{pmatrix} 0 & H_b^0 \\ -(H_b^0)^T & C_b \end{pmatrix} \begin{pmatrix} \frac{\partial \mathcal{H}}{\partial H_b^0} \\ \frac{\partial \mathcal{H}}{\partial P_b^b} \end{pmatrix} + \begin{pmatrix} 0 \\ I_6 \end{pmatrix} W_b^b \\ T_b^{b,0} &= \begin{pmatrix} 0 & I_6 \end{pmatrix} \begin{pmatrix} \frac{\partial \mathcal{H}}{\partial H_b^0} \\ \frac{\partial \mathcal{H}}{\partial P_b^b} \end{pmatrix} \end{aligned} \tag{2.53}$$

Dampers

Dampers do not have a state since they do not store energy, they only dissipate it. Note that energy is not "destroyed" in the dampers but transformed into thermal energy. This can be modelled with a thermal port connected to the environment. For reasons of simplicity the generated thermal energy is discarded. The easiest way to achieve damping is a linear resistive element D, such that the wrench is directly proportional to twist. Consider for example a body's motion with respect to the inertial frame

$$W_b^b = D T_b^{b,0} \tag{2.54}$$

Or a damper in parallel with spring

$$W_i^{j,j} = D T_i^j \tag{2.55}$$

The dissipated co-energy is $E_D = \frac{1}{2} T^T D T$.

2.4 Spring-mass-damper systems in 3D space

Recall the motivating example from Section 2.2 of a simple spring-mass system. We can add a damper d to eq. (2.7)

$$\begin{pmatrix}\dot{q}\\ \dot{p}\end{pmatrix} = \begin{pmatrix}0 & 1\\ -1 & -d\end{pmatrix}\begin{pmatrix}\frac{\partial \mathcal{H}}{\partial q}(q,p)\\ \frac{\partial \mathcal{H}}{\partial p}(q,p)\end{pmatrix} + \begin{pmatrix}0\\ 1\end{pmatrix} F_e \tag{2.56}$$

This is the port-Hamiltonian representation of a one-dimensional spring-mass-damper system. Connecting two masses by a spring and a parallel damper is a simple model for a compliant contact [DS09]. Moreover spring-mass-damper systems are the basis of the virtual structures that form the controllers in section 2.6. In cooperative object manipulation there are two compliant contact situations. One to realize soft interaction between object and environment, i.e. actual and desired object position are impedance controlled (see also the related work section). The other is the object-manipulator connection.
The derivation of the sprang-mass-damper system starts from an inertia, which is subject to gravity as modelled in eq. (2.53). Another spring is added to the inertia associated with Ψ_b. This spring connects to a desired object position assigned to Ψ_v. Its port-Hamiltonian representation is given by

$$\begin{aligned}\dot{H}_b^v &= H_b^v T_b^{b,v}\\ W_b^{b,v} &= (H_b^v)^T \frac{\partial V_{\mathrm{P}}(H_b^v)}{\partial H_b^v}\end{aligned} \tag{2.57}$$

The deformation twist of the spring is decomposed by $T_b^{b,v} = T_b^{b,0} - T_v^{b,0}$. The damping along this spring is $W_b^b = D_b T_b^{b,v}$. Mass, spring and damper move uniformly with the twist $T_b^{b,0}$ and the wrenches add up. Combining all components one obtains

$$\begin{pmatrix}\dot{H}_b^0\\ \dot{H}_b^v\\ \dot{P}_b^b\end{pmatrix} = \begin{pmatrix}0 & 0 & H_b^0\\ 0 & 0 & H_b^v\\ -(H_b^0)^T & -(H_b^v)^T & C_b - D_b\end{pmatrix}\begin{pmatrix}\frac{\partial \mathcal{H}}{\partial H_b^0}\\ \frac{\partial \mathcal{H}}{\partial H_b^v}\\ \frac{\partial \mathcal{H}}{\partial P_b^b}\end{pmatrix} + \begin{pmatrix}0 & 0\\ -H_b^v Ad_{H_0^b} & 0\\ D_b Ad_{H_0^b} & I_6\end{pmatrix}\begin{pmatrix}T_v^0\\ W_b^b\end{pmatrix}$$
$$\begin{pmatrix}W_v^{0,0}\\ T_b^{b,0}\end{pmatrix} = \begin{pmatrix}0 & -Ad^T_{H_0^b}(H_b^v)^T & Ad^T_{H_0^b} D_b\\ 0 & 0 & I_6\end{pmatrix}\begin{pmatrix}\frac{\partial \mathcal{H}}{\partial H_b^0}\\ \frac{\partial \mathcal{H}}{\partial H_b^v}\\ \frac{\partial \mathcal{H}}{\partial P_b^b}\end{pmatrix} \tag{2.58}$$

This clearly accounts for an *external* impedance relation, used to establish compliant behaviour between (virtual) object and environment. Analogously one can define impedance relations between manipulators and virtual object. To this purpose a manipulator inertia is introduced and connected to the object with a spring and a damper. Here the manipulator masses are considered gravity pre-compensated and the spring connecting to the ground is omitted. This reduces complexity in the

following. The i-th manipulator inertia is given by

$$\begin{aligned} \dot{P}_i^i &= C_i \frac{\partial V_{\mathrm{K}}(P_i^i)}{\partial P_i^i} + I_6 W_i^i \\ T_i^{i,0} &= I_6 \frac{\partial V_{\mathrm{K}}(P_i^i)}{\partial P_i^i} \end{aligned} \tag{2.59}$$

It is important that the spring connecting b and i does not connect to the center of the object b but to a point $b(i)$ on the surface of b. Clearly the distance $\boldsymbol{p}_{b(i)}^b$ corresponds to the extent of the object. The spring's twist decomposes as follows

$$T_{b(i)}^i = T_b^i + T_{b(i)}^{i,b} = Ad_{H_b^i} T_b^{b,0} - T_i^{i,0} + Ad_{H_b^i} \underbrace{T_{b(i)}^b}_{=0} \tag{2.60}$$

The spring is given by

$$\begin{aligned} \dot{H}_{b(i)}^i &= H_{b(i)}^i \begin{pmatrix} Ad_{H_b^{b(i)}} & -Ad_{H_i^{b(i)}} \end{pmatrix} \begin{pmatrix} T_b^{b,0} \\ T_i^{i,0} \end{pmatrix} \\ \begin{pmatrix} W_b^{b,0} \\ W_i^{i,0} \end{pmatrix} &= \begin{pmatrix} Ad^T_{H_b^{b(i)}} \\ -Ad^T_{H_i^{b(i)}} \end{pmatrix} (H_{b(i)}^i)^T \frac{\partial V_{\mathrm{P}}(H_b^{b(i)})}{\partial H_{b(i)}^i} \end{aligned} \tag{2.61}$$

and the damper along the spring exerts a wrench on the body i

$$W_i^i = D_i T_i^{i,b} = D_i T_i^{i,0} - D_i Ad_{H_b^i} T_b^{b,0}. \tag{2.62}$$

We can combine spring, inertia and damper. The twist $T_i^{i,0}$ is the common quantity.

$$\begin{aligned} \begin{pmatrix} \dot{H}_{b(i)}^i \\ \dot{P}_i^i \end{pmatrix} &= \begin{pmatrix} 0 & -H_{b(i)}^i Ad_{H_i^{b(i)}} \\ Ad^T_{H_i^{b(i)}} (H_{b(i)}^i)^T & C_i - D_i \end{pmatrix} \begin{pmatrix} \frac{\partial \mathcal{H}}{\partial H_{b(i)}^i} \\ \frac{\partial \mathcal{H}}{\partial P_i^i} \end{pmatrix} \\ &\quad + \begin{pmatrix} H_{b(i)}^i Ad_{H_b^{b(i)}} & 0 \\ D_i Ad_{H_b^i} & I_6 \end{pmatrix} \begin{pmatrix} T_b^{b,0} \\ W_i^i \end{pmatrix} \\ \begin{pmatrix} W_b^{b,0} \\ T_i^{i,0} \end{pmatrix} &= \begin{pmatrix} Ad^T_{H_b^{b(i)}} (H_{b(i)}^i)^T & Ad^T_{H_b^i} D_i^T \\ 0 & I_6 \end{pmatrix} \begin{pmatrix} \frac{\partial \mathcal{H}}{\partial H_{b(i)}^i} \\ \frac{\partial \mathcal{H}}{\partial P_i^i} \end{pmatrix} \end{aligned} \tag{2.63}$$

2.5 Imposing constraints

The interconnection of a spring and an inertia is the ideal pair in terms of input-output causality. The spring expects a twist-input and outputs a wrench. The inertia has a wrench-input and outputs a twist. It can be seen from eq. (2.53) that the interconnection of inertia and spring gives a set of ordinary differential equations (ODEs). Many mechanical systems cannot be modelled by an interconnection

of springs and masses. The prime example is the contact of two rigid objects. Rigid means there is no elastic deformation to be modelled by a spring (for an extensive treatment of hard and soft contact see [DS09]). Rigidly connected objects cannot move with respect to each other, i.e. they move uniformly. In cooperative manipulation the manipulators often are rigidly connected to the common object. The attempt to move the bodies individually results in *internal* forces. A force is termed internal if it produces no *virtual work* with the system's velocity (see [EH16] for a formal definition). The motion-limiting conditions are called kinematic *constraints* and are expressed in the form

$$A^T(\boldsymbol{q})\dot{\boldsymbol{q}} = 0, \tag{2.64}$$

where $A(\boldsymbol{q}) \in \mathbb{R}^{k\times l}$ is the *constraint* matrix and l being the number of independent kinematic constraints. The derivation of the constrained Hamiltonian equations starts from the Euler-Lagrange equations of constrained motion [DMSB09]

$$\begin{aligned} \frac{d}{dt}\left(\frac{\partial \mathcal{L}}{\partial \dot{\boldsymbol{q}}}\right) - \frac{\partial \mathcal{L}}{\partial \boldsymbol{q}} &= G(\boldsymbol{q})\boldsymbol{u} + A(\boldsymbol{q})\boldsymbol{\lambda} \\ A^T(\boldsymbol{q})\dot{\boldsymbol{q}} &= 0 \end{aligned} \tag{2.65}$$

The associated constraint forces are given by $A(\boldsymbol{q})\boldsymbol{\lambda}$, where $\boldsymbol{\lambda} \in \mathbb{R}^l$ are the *Lagrange* multipliers. They are uniquely determined if the constraints are satisfied, i.e. are given by the requirement $A^T(\boldsymbol{q})\dot{\boldsymbol{q}} = 0$. In this case the constraint forces do not influence the energy of the system since $\boldsymbol{\lambda}^T(A^T(\boldsymbol{q})\dot{\boldsymbol{q}}) = 0$, this corresponds to the requirement of a zero virtual work for internal forces. Similarly to Section 2.2, the Euler-Lagrange equations can be transformed to a port-Hamiltonian equivalent, which is a mixed set of differential and algebraic equations (DAE).

$$\begin{aligned} \begin{pmatrix} \dot{\boldsymbol{q}} \\ \dot{\boldsymbol{p}} \end{pmatrix} &= \begin{pmatrix} 0 & I \\ -I & 0 \end{pmatrix} \begin{pmatrix} \frac{\partial \mathcal{H}}{\partial \boldsymbol{q}} \\ \frac{\partial \mathcal{H}}{\partial \boldsymbol{p}} \end{pmatrix} + \begin{pmatrix} 0 & 0 \\ A(\boldsymbol{q}) & G(\boldsymbol{q}) \end{pmatrix} \begin{pmatrix} \boldsymbol{\lambda} \\ \boldsymbol{u} \end{pmatrix} \\ \begin{pmatrix} 0 \\ e \end{pmatrix} &= \begin{pmatrix} 0 & A^T(\boldsymbol{q}) \\ 0 & G^T(\boldsymbol{q}) \end{pmatrix} \begin{pmatrix} \frac{\partial \mathcal{H}}{\partial \boldsymbol{p}} \\ \frac{\partial \mathcal{H}}{\partial \boldsymbol{p}} \end{pmatrix} \end{aligned} \tag{2.66}$$

The system is no longer described in the input-state-output form. The additional condition to be fulfilled brings the system to a semi-explicit form [vdS13]. Several approaches to solve the algebraic equations and restore the desired input-state-output form exist. Most of them are designed for generalized configuration $\boldsymbol{q}$ and momentum $\boldsymbol{p}$ coordinates, see e.g. [vdS13],[DS09]. Due to non-linearity of $\dot{\boldsymbol{q}} = \frac{\partial \mathcal{H}}{\partial \boldsymbol{p}}$ in mechanical systems not all are feasible for 3D mechanical systems.
The following method (described e.g. in [DS09]) uses the time-derivative of the constraints

$$0 = \frac{d}{dt}\left(A^T(\boldsymbol{q})\frac{\partial \mathcal{H}}{\partial \boldsymbol{p}}\right) \tag{2.67}$$

We use the property $\frac{\partial \mathcal{H}}{\partial \boldsymbol{p}} = M^{-1}\boldsymbol{p}$ for an energy function of the form $\mathcal{H} = \frac{1}{2}\boldsymbol{p}^T M^{-1}\boldsymbol{p} + V_{\mathrm{P}}$. Since $\boldsymbol{q}(t)$ is time-variant *indirect dependencies* arise in $A(\boldsymbol{q})$ and $\boldsymbol{p}(\boldsymbol{q})$ when

calculating the total time-derivative

$$\begin{aligned} 0 = \frac{d}{dt}(A^T M^{-1}\boldsymbol{p}) &= \frac{\partial(A^T M^{-1}\boldsymbol{p})}{\partial \boldsymbol{q}}\dot{\boldsymbol{q}} + A^T M^{-1}\dot{\boldsymbol{p}} \\ &= \frac{\partial(A^T M^{-1}\boldsymbol{p})}{\partial \boldsymbol{q}} M^{-1}\boldsymbol{p} + A^T M^{-1}\left(-\frac{\partial \mathcal{H}}{\partial \boldsymbol{q}} + A(\boldsymbol{q})\boldsymbol{\lambda} + G(\boldsymbol{q})\boldsymbol{u}\right) \end{aligned} \tag{2.68}$$

Solving this equation for $\boldsymbol{\lambda}$ gives an analytic expression for the constrained forces

$$\boldsymbol{\lambda} = (A^T M^{-1} A)^{-1}\left(-\frac{\partial(A^T M^{-1} p)}{\partial \boldsymbol{q}} M^{-1}\boldsymbol{p} + \frac{\partial \mathcal{H}}{\partial \boldsymbol{q}} - G\boldsymbol{u}\right) \tag{2.69}$$

After the re-insertion of $\boldsymbol{\lambda}$ into eq. (2.66), one obtains a set of ODEs in input-state-output form. Clearly the term $A(\boldsymbol{q})\boldsymbol{\lambda}$ generates internal forces, that oppose relative motions of the bodies and keep the constraints $A^T(\boldsymbol{q})\dot{\boldsymbol{q}}$ fulfilled. Since the computation of the constraint forces starts from the time-derivative of the constraints, $A^T(\boldsymbol{q})\dot{\boldsymbol{q}}$ remains constant. To guarantee $A^T(\boldsymbol{q})\dot{\boldsymbol{q}} = 0$, this must be fulfilled in the beginning, e.g. by a not-moving system $\dot{\boldsymbol{q}}(0) = 0$.

Constraints for 6D-motion

Consider two rigidly connected bodies, associated with the frames Ψ_b and Ψ_i and a distance between them $\boldsymbol{p}_i^b = \boldsymbol{p}_i^0 - \boldsymbol{p}_b^0$. Clearly, in the setting of cooperative manipulation, one can think of an object b and the i-th manipulator attached to it. Now let the body b rotate with the angular velocity $\boldsymbol{\omega}_b^0$. Being rigidly attached the body i rotates in the same manner, $\boldsymbol{\omega}_i^0 = \boldsymbol{\omega}_b^0$. The translational velocity of body i is expressed dependent on body b by

$$\begin{aligned} \dot{\boldsymbol{p}}_i^0 &= \dot{\boldsymbol{p}}_b^0 + \boldsymbol{\omega}_b^0 \times \boldsymbol{p}_i^b = \dot{\boldsymbol{p}}_b^0 + \boldsymbol{\omega}_b^0 \times (\boldsymbol{p}_i^0 - \boldsymbol{p}_b^0) \\ \dot{\boldsymbol{p}}_i^0 - \boldsymbol{\omega}_b^0 \times \boldsymbol{p}_i^0 &= \dot{\boldsymbol{p}}_b^0 - \boldsymbol{\omega}_b^0 \times \boldsymbol{p}_b^0 \end{aligned} \tag{2.70}$$

Recall the definition of the linear velocity component of a twist from eq. (2.30) being $\boldsymbol{v}_i^j = \dot{\boldsymbol{p}}_i^j - \boldsymbol{\omega}_i^j \times \boldsymbol{p}_i^j$. Thus the velocities $\boldsymbol{v}_i^0 = \boldsymbol{v}_b^0$ are equal and consequently the twists $T_i^0 = T_b^0$ are equal as well. For a system of $i = 1...N$ manipulators we write the constraints

$$0 = A^T T = \begin{pmatrix} -I_3 & 0_3 & I_3 & 0_3 & & & \\ 0_3 & -I_3 & 0_3 & I_3 & & & \\ \vdots & \vdots & & & \ddots & & \\ -I_3 & 0_3 & & & & I_3 & 0_3 \\ 0_3 & -I_3 & & & & 0_3 & I_3 \end{pmatrix} \begin{pmatrix} T_b^0 \\ T_1^0 \\ \vdots \\ T_N^0 \end{pmatrix} \tag{2.71}$$

The elimination of the algebraic condition starts by differentiating the constraints, here A is not time or configuration dependent, thus $0 = A^T \dot{T}$. Consider the simple

example of two rigidly connected bodies b and i. The constraint equation is

$$\begin{aligned} 0 = \dot{T}_i^0 - \dot{T}_b^0 = \begin{pmatrix} \dot{\boldsymbol{\omega}}_i^0 - \dot{\boldsymbol{\omega}}_b^0 \\ \dot{\boldsymbol{v}}_i^0 - \dot{\boldsymbol{v}}_b^0 \end{pmatrix} = \begin{pmatrix} \dot{\boldsymbol{\omega}}_i^0 - \dot{\boldsymbol{\omega}}_b^0 \\ \frac{d}{dt}(\dot{\boldsymbol{p}}_i^0 - \boldsymbol{\omega}_b^0 \times \boldsymbol{p}_i^0) - \frac{d}{dt}(\dot{\boldsymbol{p}}_b^0 - \boldsymbol{\omega}_b^0 \times \boldsymbol{p}_b^0) \end{pmatrix} \\ = \begin{pmatrix} \dot{\boldsymbol{\omega}}_i^0 - \dot{\boldsymbol{\omega}}_b^0 \\ \ddot{\boldsymbol{p}}_i^0 - \ddot{\boldsymbol{p}}_b^0 - \dot{\boldsymbol{\omega}}_b^0 \times \boldsymbol{p}_i^b - \boldsymbol{\omega}_b^0 \times (\boldsymbol{\omega}_b^0 \times \boldsymbol{p}_i^b) \end{pmatrix} \end{aligned} \tag{2.72}$$

Kinematic constraints are expressed very compactly in the twist notation. Second-order dynamics including *centripetal* terms are inherent and equivalent to classic representations (see e.g.[EH16]).
Towards solving the set of port-Hamiltonian DAEs, recall from equation (2.66) that $0 = A^T \frac{\partial \mathcal{H}}{\partial \boldsymbol{p}}$. At this point it is necessary to distinguish different twist representations, e.g. $\frac{\partial \mathcal{H}}{\partial P_b^b} = T_b^{b,0} = Ad_{H_0^b} T_b^0$. Continuing the two mass example the constraints are re-written

$$0 = A^T \begin{pmatrix} T_b^0 \\ T_i^0 \end{pmatrix} = \underbrace{A^T \begin{pmatrix} Ad_{H_b^0} & 0 \\ 0 & Ad_{H_i^0} \end{pmatrix}}_{\bar{A}^T} \begin{pmatrix} T_b^{b,0} \\ T_i^{i,0} \end{pmatrix} = A^T \begin{pmatrix} Ad_{H_b^0} & 0 \\ 0 & Ad_{H_i^0} \end{pmatrix} \begin{pmatrix} \frac{\partial \mathcal{H}}{\partial P_b^b} \\ \frac{\partial \mathcal{H}}{\partial P_i^i} \end{pmatrix} \tag{2.73}$$

Replacing the twists with momenta $T = M^{-1}P$ and differentiating w.r.t to time leads to

$$0 = \bar{A}^T \begin{pmatrix} M_b^{-1} & 0 \\ 0 & M_i^{-1} \end{pmatrix} \begin{pmatrix} \dot{P}_b^b \\ \dot{P}_i^i \end{pmatrix} + \bar{A}^T \begin{pmatrix} ad_{T_b^{b,0}} & 0 \\ 0 & ad_{T_i^{i,0}} \end{pmatrix} \begin{pmatrix} M_b^{-1} & 0 \\ 0 & M_i^{-1} \end{pmatrix} \begin{pmatrix} P_b^b \\ P_i^i \end{pmatrix} \tag{2.74}$$

Consider now the last part of this equation and recall the adjoint representation ad_T from eq. (2.44). One obtains for body b

$$ad_{T_b^{b,0}} M_b^{-1} P_b^b = \begin{pmatrix} \tilde{\omega}_b^{b,0} & 0 \\ \tilde{v}_b^{b,0} & \tilde{\omega}_b^{b,0} \end{pmatrix} \begin{pmatrix} \boldsymbol{\omega}_b^{b,0} \\ \boldsymbol{v}_b^{b,0} \end{pmatrix} = 0 \tag{2.75}$$

Here the inertias are assumed to be not configuration dependent, i.e. time-invariant. A real robot has multiple joints and link, its effective inertia is thus configuration dependent. Feedback-linearisation techniques [OASK+04] compensate for the internal dynamic in favour of shaping a desired inertia. The assumption of a non-configuration dependent manipulation inertia is reasonable, if a perfect feedback-linearisation is implemented on the robot. Then the insertion of the port-Hamiltonian system equation for $\dot{P}$ leads to

$$0 = \bar{A}^T M^{-1} \dot{P} = \bar{A}^T M^{-1} (W + CT + \bar{A}\lambda) \tag{2.76}$$

and solve for λ

$$\lambda = -(\bar{A}^T M^{-1} \bar{A})^{-1} \bar{A}^T M^{-1} (W + CT) \tag{2.77}$$

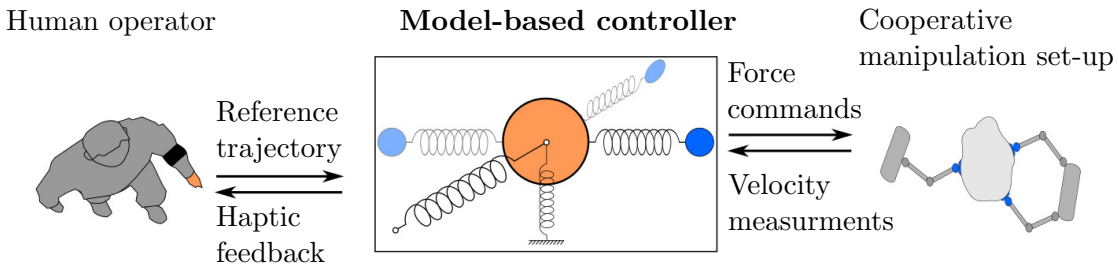

Figure 2.4: The model-based controller virtually links human and robots

Consider again the example of two rigidly connected bodies b and i. Let us examine the part $\bar{A}^T M^{-1} C T$ in further detail. Using eq. (2.46) and assuming that the bodies share the orientation $R_0^b = R_0^i$, one obtains

$$\begin{aligned} \bar{A}^T M^{-1} \begin{pmatrix} C_b T_b^{b,0} \\ C_i T_i^{i,0} \end{pmatrix} &= \bar{A}^T M^{-1} \begin{pmatrix} 0 \\ m_b \tilde{v}_b^{b,0} \boldsymbol{\omega}_b^{b,0} \\ 0 \\ m_i \tilde{v}_i^{i,0} \boldsymbol{\omega}_b^{b,0} \end{pmatrix} = \begin{pmatrix} -I_6 & I_6 \end{pmatrix} \begin{pmatrix} 0 \\ R_b^0 \tilde{v}_b^{b,0} \boldsymbol{\omega}_b^{b,0} \\ 0 \\ R_b^0 \tilde{v}_i^{i,0} \boldsymbol{\omega}_b^{b,0} \end{pmatrix} \\ &= \begin{pmatrix} 0 \\ R_b^0 \tilde{\omega}_b^{b,0} (\tilde{p}_0^b R_b^0 \boldsymbol{\omega}_b^0 + R_0^b \boldsymbol{v}_b^0 - \tilde{p}_0^i R_0^b \boldsymbol{\omega}_b^0 - R_0^b \boldsymbol{v}_i^0) \end{pmatrix} = \begin{pmatrix} 0 \\ R_b^0 \tilde{\omega}_b^{b,0} \tilde{p}_i^b \boldsymbol{\omega}_b^{b,0} \end{pmatrix} \end{aligned} \tag{2.78}$$

This example shows how kinematic constraints can be solved by calculating the constraint forces. The results are equivalent to approaches based on the *Gauss' principle of least constraint* ([EH16]) or *Euler-Lagrange* representations ([LL02]).

2.6 Model-based controllers for cooperative manipulation

In this section two model-based control schemes are designed by building virtual structures to achieve a certain group behaviour of the robots. This approach can be viewed in the context of formation control and is also very similar to the *Intrinsically Passive Controller* (IPC) paradigm introduced by Stramigioli [Str01b]. It has the advantages of a physical fundament, passivity and stability during contact and non-contact transitions. Please note that the controller is no more than a geometric interconnection of mechanic elements in a virtual domain.

One approach to establish a desired formation of robots is connecting them with virtual springs and dampers. The IPC furthermore introduces a virtual object. The proposed controller design mimics an impedance controlled cooperative manipulation set-up, i.e. the controller has the structure of robots manipulating a common object, see figure 2.4 for an overview.

In this *virtual* set-up the common object and the manipulators are simple inertias. The manipulators connect to the object by springs and dampers, i.e. the connection

is compliant. This leads to stability during contact and non-contact transitions.
The scheme is object-centred, i.e. the user controls the object directly and the controller generates appropriate commands for the robotic system. Direct here refers to a virtual coupling between the user (i.e. the reference trajectory given by the user) and the virtual object, established by a spring and a damper.
The robots connect to the virtual object equally with a spring and a damper. Therefore the formation is established autonomously. The control output to the robots is either a reference trajectory (subsection 2.6.1) or force commands (subsection 2.6.2). The respective dual quantity serves as an input for the controller.
Conclusively the controller is a virtual system model that generates control outputs by simulating the dynamics of its internal structure. Every connection either between the sub-elements inside the controller or the external ones (user-controller, controller-robots) are described by effort-flow pairs, i.e. power ports. From an energetic point of view the interconnection is lossless (see subsection 2.2.1) and the elements are passive. This motivates the term *intrinsic passivity* [Str01b]. By definition a passive controller cannot generate energy, thus energy must be provided from outside, either by the user or by the robotic system, through the power ports. Stramigioli's original IPC scheme [Str01b] does not incorporate the inertias of the manipulators, nor damping along the manipulator springs, in the controller. For the energy shaping control applied in chapter 3 an exact model of the cooperative set-up is necessary. The manipulator inertias can be added to the controller in (at least) two ways, leading to the two schemes presented below.

2.6.1 Compliant trajectory generating dynamic IPC

Beginning from the mechanical impedance equations derived in subsection 2.4, a controller based on the structure of the cooperative manipulation set-up is designed. The starting point is the impedance equation (2.58) accounting for the relation between object and reference trajectory. The inertia M_b represents the common object, spring and damper establish a relation between desired and *actual* object twist. In this context the actual twist is the twist of the simulated object (no object tracking information from the real set-up is used). Analogously to a real cooperative manipulation set-up, the n-manipulators connect to the virtual object. In the controller these connections are compliant (not rigid), i.e. springs are between object and manipulators. The manipulator-object impedance equation (2.63) defines the springs, mass and dampers of the modelled manipulators. One spring hinge-point is connected to the surface of the object, the other hinge point is connected to the virtual inertia M_i, which clearly represents the i-th manipulator's body. In summary a simple geometric interconnection of the impedance equations (2.58,2.63) forms the controller. The structure can be seen from figure 2.5. In place of a full cooperative manipulation set-up with n manipulators, the derivation of the controller is shown for a single manipulator i.

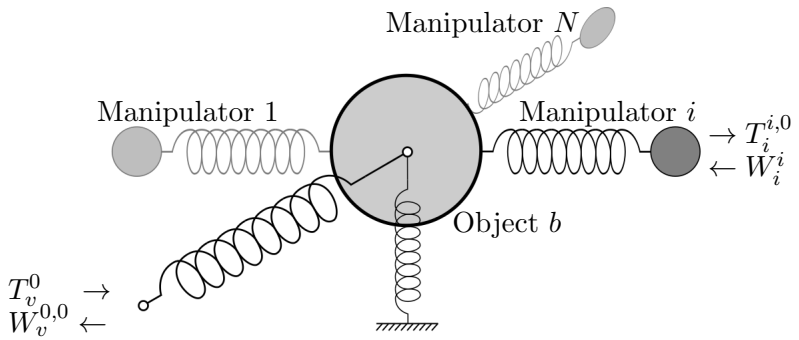

Figure 2.5: Virtual structure connecting operator and robots in the compliant reference trajectory generating controller

$$\begin{pmatrix} \dot{H}_b^0 \\ \dot{H}_b^v \\ \dot{P}_b^b \\ \dot{H}_{b(i)}^i \\ \dot{P}_i^i \end{pmatrix} = \begin{pmatrix} 0 & 0 & H_b^0 & 0 & 0 \\ 0 & 0 & H_b^v & 0 & 0 \\ -H_b^{0T} & -H_b^{vT} & C_b - D_b & -Ad^T_{H_b^{b(i)}} {H_{b(i)}^i}^T & -Ad^T_{H_b^i} D_i \\ 0 & 0 & H_{b(i)}^i Ad_{H_b^{b(i)}} & 0 & -H_{b(i)}^i Ad_{H_i^{b(i)}} \\ 0 & 0 & D_i Ad_{H_b^i} & Ad^T_{H_i^{b(i)}} {H_{b(i)}^i}^T & C_i - D_i \end{pmatrix} \begin{pmatrix} \frac{\partial \mathcal{H}}{\partial H_b^0} \\ \frac{\partial \mathcal{H}}{\partial H_b^v} \\ \frac{\partial \mathcal{H}}{\partial P_b^b} \\ \frac{\partial \mathcal{H}}{\partial H_{b(i)}^i} \\ \frac{\partial \mathcal{H}}{\partial P_i^i} \end{pmatrix} + \begin{pmatrix} 0 & 0 \\ -H_b^v Ad_{H_0^b} & 0 \\ D_b Ad_{H_0^b} & 0 \\ 0 & 0 \\ 0 & I_6 \end{pmatrix} \begin{pmatrix} T_v^0 \\ W_i^i \end{pmatrix} \tag{2.79}$$

$$\begin{pmatrix} W_v^{0,0} \\ T_i^{i,0} \end{pmatrix} = \begin{pmatrix} 0 & -Ad^T_{H_0^b} H_b^{vT} & Ad^T_{H_0^b} D_b^T & 0 & 0 \\ 0 & 0 & 0 & 0 & I_6 \end{pmatrix} \begin{pmatrix} \frac{\partial \mathcal{H}}{\partial H_b^0} \\ \frac{\partial \mathcal{H}}{\partial H_b^v} \\ \frac{\partial \mathcal{H}}{\partial P_b^b} \\ \frac{\partial \mathcal{H}}{\partial H_{b(i)}^i} \\ \frac{\partial \mathcal{H}}{\partial P_i^i} \end{pmatrix}$$

Note that the control output generated by this controller is twist, i.e. a compliant reference trajectory for the robots to follow. Similar to [CCMV08] we require a local (on joint level) underlying force control layer to operate the robots.

Passivity

Passivity follows directly from the port-Hamiltonian formulation.

Proof. The above representation is of the standard from (2.11). The terms to be omitted due to the skew-symmetry of the structure matrix $J(x)$ are not given in the

following energy balance

$$\begin{aligned}\dot{\mathcal{H}} &= -\frac{\partial^T \mathcal{H}}{\partial P_b^b} D_b \frac{\partial \mathcal{H}}{\partial P_b^b} - \frac{\partial^T \mathcal{H}}{\partial P_i^i} D_i \frac{\partial \mathcal{H}}{\partial P_i^i} \\ &- \frac{\partial^T \mathcal{H}}{\partial H_b^v} H_b^v Ad_{H_0^b} T_v^0 + \frac{\partial^T \mathcal{H}}{\partial P_b^b} D_b Ad_{H_0^b} T_v^0 + \frac{\partial^T \mathcal{H}}{\partial P_i^i} W_i^i \\ &= \underbrace{-\frac{\partial^T \mathcal{H}}{\partial P_b^b} D_b \frac{\partial \mathcal{H}}{\partial P_b^b} - \frac{\partial^T \mathcal{H}}{\partial P_i^i} D_i \frac{\partial \mathcal{H}}{\partial P_i^i}}_{\text{dissipation}} + \underbrace{W_v^{0,0^T} T_v^0 + T_i^{i,0^T} W_i^i}_{\text{inputs}},\end{aligned} \tag{2.80}$$

i.e. the controller is passive. This is a sufficient condition for asymptotic stability. □

2.6.2 Constrained dynamics IPC

In the compliant trajectory generating IPC, the virtual manipulator inertia connects to the virtual object by a spring. It is also possible to directly connect the two inertias. Typically in a real cooperative set-up the manipulator-object connection is assumed rigid. This requires the modelling of a rigid contact as treated in section 2.5. Another advantage of the constrained dynamics controller is that a measurement of the end-effector forces is unnecessary. Generally robots are equipped with rotary encoders measuring the joint angles and -velocities. Employing forward kinematics the end-effector velocity is obtained without an additional sensor. In contrast to this the effective end-effector wrench can only be obtained by measurement with force/torque sensors. From this point of view it is convenient to design a controller that issues force commands to the robots and receives velocity feedback. The difficulty to overcome here is the *preferred causality* of port-Hamiltonian elements. Please note from subsection 2.3.3 that springs expect a twist for input and output a wrench. Vice versa inertias accept a wrench input, resulting in a twist output. In this formulations the state variable is computed by integration over time, opposite causality representations are possible but require the time derivative. Numerical differentiation amplifies numerical noise, thus the integration form is the preferred one. Furthermore integration allows to use information in form of initial conditions, while differentiation does not. For more information on causality see [DMSB09].
In the controller both the virtual object and the robotic system expect wrenches, in terms of causality calling for a spring. Therefore a virtual manipulator inertia is added by rigidly connecting it to the virtual object, figure 2.6 illustrates the composition. In a real cooperative manipulation set-up it is also common to have this rigid connection between end-effector and object, making this an obvious choice for control.
Rigid coupling of a manipulator and the object is treated with the approach presented in section 2.5. Once again the derivation starts from a single manipulator i in place of a full cooperative manipulation set-up. Bodies b and $b(i)$ are rigidly

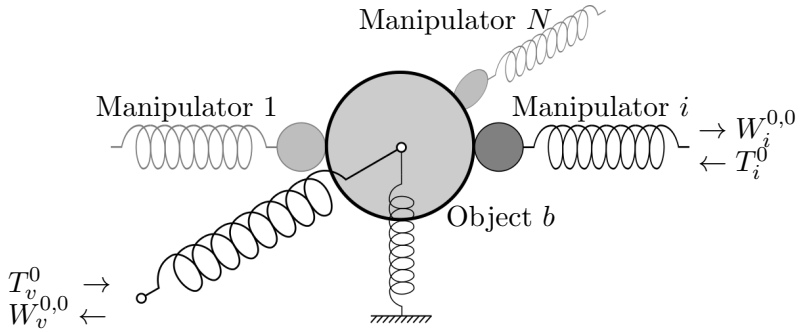

Figure 2.6: Structure of the constrained dynamic IPC

connected and their port-Hamiltonian equations are

$$\begin{aligned}\begin{pmatrix}\dot{P}_b^b\\ \dot{P}_{b(i)}^{b(i)}\end{pmatrix} &= \begin{pmatrix}C_b & 0\\ 0 & C_{b(i)}\end{pmatrix}\begin{pmatrix}\frac{\partial \mathcal{H}}{\partial P_b^b}\\ \frac{\partial \mathcal{H}}{\partial P_{b(i)}^{b(i)}}\end{pmatrix} + \begin{pmatrix}W_b^b\\ W_{b(i)}^{b(i)}\end{pmatrix} + \bar{A}\boldsymbol{\lambda}\\ 0 &= \bar{A}^T\begin{pmatrix}\frac{\partial V}{\partial P_b^b}\\ \frac{\partial V}{\partial P_{b(i)}^{b(i)}}\end{pmatrix}\end{aligned} \tag{2.81}$$

The Lagrange multipliers are eliminated as shown in section 2.5. In order to write the full control scheme in a compact notation, four abbreviations account for the constrained forces

$$\begin{aligned}\mathcal{A}_b^b &= Ad_{H_b^0}^T(\bar{A}^T M^{-1}\bar{A})^{-1}Ad_{H_b^0}M_b^{-1}\\ \mathcal{A}_b^i &= Ad_{H_b^0}^T(\bar{A}^T M^{-1}\bar{A})^{-1}Ad_{H_{b(i)}^0}M_{b(i)}^{-1}\\ \mathcal{A}_i^b &= Ad_{H_{b(i)}^0}^T(\bar{A}^T M^{-1}\bar{A})^{-1}Ad_{H_b^0}M_b^{-1}\\ \mathcal{A}_i^i &= Ad_{H_{b(i)}^0}^T(\bar{A}^T M^{-1}\bar{A})^{-1}Ad_{H_{b(i)}^0}M_{b(i)}^{-1}\end{aligned} \tag{2.82}$$

$$\begin{aligned}\begin{pmatrix}\dot{H}_b^0\\ \dot{H}_b^v\\ \dot{P}_b^b\\ \dot{H}_{b(i)}^i\\ \dot{P}_{b(i)}^{b(i)}\end{pmatrix} &= \begin{pmatrix}0 & 0 & H_b^0 & 0 & 0\\ 0 & 0 & H_b^v & 0 & 0\\ (\mathcal{A}_b^b - I)H_b^{0T} & (\mathcal{A}_b^b - I)H_b^{vT} & (I-\mathcal{A}_b^b)(C_b - D_b) & -\mathcal{A}_b^i {H_{b(i)}^i}^T & \mathcal{A}_b^i(C_{b(i)} - D_{b(i)})\\ 0 & 0 & 0 & 0 & H_{b(i)}^i\\ -\mathcal{A}_i^b H_b^{0T} & -\mathcal{A}_i^b H_b^{vT} & \mathcal{A}_i^b(C_b - D_b) & (\mathcal{A}_i^i - I){H_{b(i)}^i}^T & (I-\mathcal{A}_i^i)(C_{b(i)} - D_{b(i)})\end{pmatrix}\begin{pmatrix}\frac{\partial V}{\partial H_b^0}\\ \frac{\partial V}{\partial H_b^v}\\ \frac{\partial V}{\partial P_b^b}\\ \frac{\partial V}{\partial H_{b(i)}^i}\\ \frac{\partial V}{\partial P_{b(i)}^{b(i)}}\end{pmatrix}\\ &+ \begin{pmatrix}0 & 0\\ -H_b^v Ad_{H_0^b} & 0\\ (I-\mathcal{A}_b^b)D_b Ad_{H_0^b} & \mathcal{A}_b^i D_{b(i)} Ad_{H_0^{b(i)}}\\ 0 & -H_{b(i)}^i Ad_{H_0^{b(i)}}\\ \mathcal{A}_i^b D_b Ad_{H_0^b} & (I-\mathcal{A}_i^i)D_{b(i)}Ad_{H_0^{b(i)}}\end{pmatrix}\begin{pmatrix}T_v^0\\ T_i^0\end{pmatrix}\end{aligned} \tag{2.83}$$

$$\begin{pmatrix}W_v^{0,0}\\ W_i^{0,0}\end{pmatrix} = \begin{pmatrix}0 & -Ad_{H_0^b}^T H_b^{vT} & Ad_{H_0^b}^T D_b^T(I-\mathcal{A}_b^{bT}) & 0 & Ad_{H_0^b}^T D_b^T \mathcal{A}_i^{bT}\\ 0 & 0 & Ad_{H_0^{b(i)}}^T D_{b(i)}^T \mathcal{A}_b^{iT} & -Ad_{H_0^{b(i)}}^T {H_{b(i)}^i}^T & Ad_{H_0^{b(i)}}^T D_{b(i)}^T(I-\mathcal{A}_i^{iT})\end{pmatrix}\begin{pmatrix}\frac{\partial V}{\partial H_b^0}\\ \frac{\partial V}{\partial H_b^v}\\ \frac{\partial V}{\partial P_b^b}\\ \frac{\partial V}{\partial H_{b(i)}^i}\\ \frac{\partial V}{\partial P_{b(i)}^{b(i)}}\end{pmatrix}$$

Passivity

In subsection 2.2.3 it is shown that skew-symmetric elements of the structure matrix (denoted with $J(x)$) do not contribute to the energy balance, i.e. are lossless. In the above equation (2.83) there is a number of elements, which neither skew-symmetric, nor dissipative. The lossless property of the interconnection still holds.

Proof. For the derivation of the energy balance the skew-symmetric elements are omitted to keep the analysis small.

$$\begin{aligned}\dot{\mathcal{H}} = &\begin{pmatrix} \frac{\partial \mathcal{H}}{\partial P_b^b} \\ \frac{\partial \mathcal{H}}{\partial P_{b(i)}^{b(i)}} \end{pmatrix}^T \begin{pmatrix} \mathcal{A}_b^b H_b^{0T} & \mathcal{A}_b^b H_b^{vT} & -\mathcal{A}_b^b(C_b - D_b) & -\mathcal{A}_b^i H_{b(i)}^{i\ T} & \mathcal{A}_b^i(C_{b(i)} - D_{b(i)}) \\ -\mathcal{A}_i^b H_b^{0T} & -\mathcal{A}_i^b H_b^{vT} & \mathcal{A}_i^b(C_b - D_b) & \mathcal{A}_i^i H_{b(i)}^{i\ T} & -\mathcal{A}_i^i(C_{b(i)} - D_{b(i)}) \end{pmatrix} \begin{pmatrix} \frac{\partial \mathcal{H}}{\partial H_b^0} \\ \frac{\partial \mathcal{H}}{\partial H_b^v} \\ \frac{\partial \mathcal{H}}{\partial P_b^b} \\ \frac{\partial \mathcal{H}}{\partial H_{b(i)}^i} \\ \frac{\partial \mathcal{H}}{\partial P_{b(i)}^{b(i)}} \end{pmatrix} \\ &- \frac{\partial^T \mathcal{H}}{\partial P_b^b} D_b \frac{\partial \mathcal{H}}{\partial P_b^b} - \frac{\partial^T \mathcal{H}}{\partial P_{b(i)}^{b(i)}} D_{b(i)} \frac{\partial \mathcal{H}}{\partial P_{b(i)}^{b(i)}} + W_v^{0,0^T} T_v^0 + W_i^{0,0^T} T_i^0 \end{aligned} \tag{2.84}$$

The bodies b and $b(i)$ are rigidly connected, i.e. their twists are related by $T_b^0 = Ad_{H_b^0} T_b^{b,0} = Ad_{H_{b(i)}^0} T_{b(i)}^{b(i),0} = T_{b(i)}^0$. In the upper equation the twists are given by $T_b^{b,0} = \frac{\partial \mathcal{H}}{\partial P_b^b}$ and $T_{b(i)}^{b(i),0} = \frac{\partial \mathcal{H}}{\partial P_{b(i)}^{b(i)}}$. Multiplying with the constraint force terms leads to

$$\begin{aligned}\frac{\partial^T \mathcal{H}}{\partial P_{b(i)}^{b(i)}} \mathcal{A}_i^b &= \frac{\partial^T \mathcal{H}}{\partial P_b^b} Ad_{H_b^{b(i)}}^T \mathcal{A}_i^b = \frac{\partial^T \mathcal{H}}{\partial P_b^b} (Ad_{H_{b(i)}^0} Ad_{H_b^{b(i)}})^T (\bar{A}^T M^{-1} \bar{A})^{-1} Ad_{H_b^0} M_b^{-1} \\ &= \frac{\partial^T \mathcal{H}}{\partial P_b^b} Ad_{H_b^0}^T (\bar{A}^T M^{-1} \bar{A})^{-1} Ad_{H_b^0} M_b^{-1} = \frac{\partial^T \mathcal{H}}{\partial P_b^b} \mathcal{A}_b^b \end{aligned} \tag{2.85}$$

and

$$\begin{aligned}\frac{\partial^T \mathcal{H}}{\partial P_{b(i)}^{b(i)}} \mathcal{A}_i^i &= \frac{\partial^T \mathcal{H}}{\partial P_b^b} Ad_{H_b^{b(i)}}^T \mathcal{A}_i^i = \frac{\partial^T \mathcal{H}}{\partial P_b^b} (Ad_{H_{b(i)}^0} Ad_{H_b^{b(i)}})^T (\bar{A}^T M^{-1} \bar{A})^{-1} Ad_{H_{b(i)}^0} M_b^{-1} \\ &= \frac{\partial^T \mathcal{H}}{\partial P_b^b} Ad_{H_b^0}^T (\bar{A}^T M^{-1} \bar{A})^{-1} Ad_{H_{b(i)}^0} M_b^{-1} = \frac{\partial^T \mathcal{H}}{\partial P_b^b} \mathcal{A}_b^i. \end{aligned} \tag{2.86}$$

The energy balance reduces to the dissipative terms and input-output pairs, the controller is thus passive.

$$\dot{\mathcal{H}} = -\frac{\partial^T \mathcal{H}}{\partial P_b^b} D_b \frac{\partial \mathcal{H}}{\partial P_b^b} - \frac{\partial^T \mathcal{H}}{\partial P_{b(i)}^{b(i)}} D_{b(i)} \frac{\partial V}{\partial P_{b(i)}^{b(i)}} + W_v^{0,0^T} T_v^0 + W_i^{0,0^T} T_i^0 \tag{2.87}$$

□

Chapter 3

Energy regulating control

Towards a conclusion on stability of the overall system, it is necessary to take the environmental conditions into consideration. Letting a human directly control a cooperative robot-team raises the question of her/his dynamic behaviour and the impact on the system. Furthermore the environment, the robotic system is interacting with, can change unexpectedly. Thus stability considerations based on certain environment models may lose their basis. Preserving stability is especially crucial when the human operator is on-site to ensure her/his safety. The objective of this chapter is to introduce an energy tank along with a suitable re-filling strategy, that sources the controller. The energy tank maintains a safe level of energy in the system, regardless of the dynamics of a human and the environment. The energy-based controllers from section 2.6 integrate seamlessly with the tank concept.

3.1 Passivity and safe energy levels

Passivity is a key concept when dealing with unknown environments. It is well known that passive robotic systems are stable with any environment, that can provide only a bounded amount of energy. On the other hand it is shown in [Str15], that for a non-passive robotic system, there always exists a (passive) environment that destabilizes the overall behaviour.
When a human operator controls a robotic set-up by hand motion, it is often argued that the human arm is not distinguishable from a mechanical impedance. This stems from experiments with a human manipulating a controlled impedance [Hog89]. The robotic device applies a force to the human and s/he responds with motion, therefore the human-machine interface is on an energetic level (the product of force and velocity is mechanical power). In recent years new input methods appeared (hand tracking, gesture control). Here the interaction between human and robotic system is an exchange of information. There is no explicit relation between force and velocity (impedance) and therefore it is not meaningful to model the human operator with an impedance. Feedback given through tactile or visual information does not effectively restrict the operator's motion, allowing him to issue nearly arbitrary com-

mands. Please recall the introductory example of a robotic system driven into an obstacle. If the user persists to command motion in the blocked direction, then an infinite amount of energy to the system can be supplied to the system. Figure 3.1 illustrates the exchange of energy of a passive robotic team with the environment and an operator, who directly powers the controller.
In order to obtain a safe and stable human-guided robotic system, the operator is assigned with an energy budget at disposal to issue commands. The structure is shown in figure 3.2 and the theory treated in the next section. This allows to achieve stability with any environment the robotic system is interacting with, as long as its energy supply is bounded. Using the concept of passivity, asymptotic stability is given without requiring certain models or assumptions for the human and the environment.
For physical human-robot interaction various safety metrics exist, see [Had14] for an overview. In this thesis the focus is limited to energy-based injury criteria. Experimental studies indicate minimal amounts of energy that cause a cranial bone failure [Woo71] or a fracture of neck bones [YPM+96]. The results provide a maximum amount of energy to be stored in the cooperative set-up

$$V_{\mathrm{K,Limit}} = \begin{cases} 517\ \mathrm{J} & \text{adult cranium bone failure} \\ 127\ \mathrm{J} & \text{infant cranium bone failure} \\ 30\ \mathrm{J} & \text{neck fracture} \end{cases} \tag{3.1}$$

The model-based controllers designed in section 2.6 simulate the energetic state of the full cooperative set-up. Assuming perfect modelling, the Hamiltonian energy function of the controller provides a value for the energy level of the real system. The control behaviour is adapted to limit the energy virtually stored in the controller. A limited amount of energy in the controller leads to a limited amount of energy in the real system. If the modelling is perfect, the energy levels are equal.

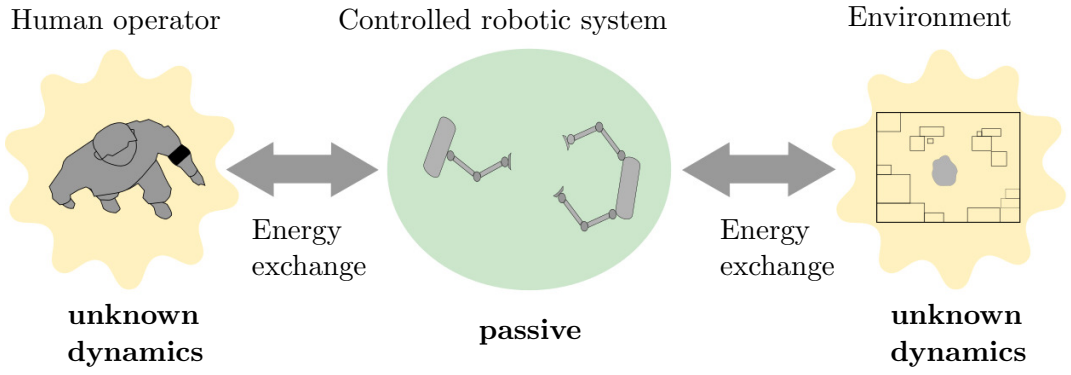

Figure 3.1: The robotic system interacting with operator and environment

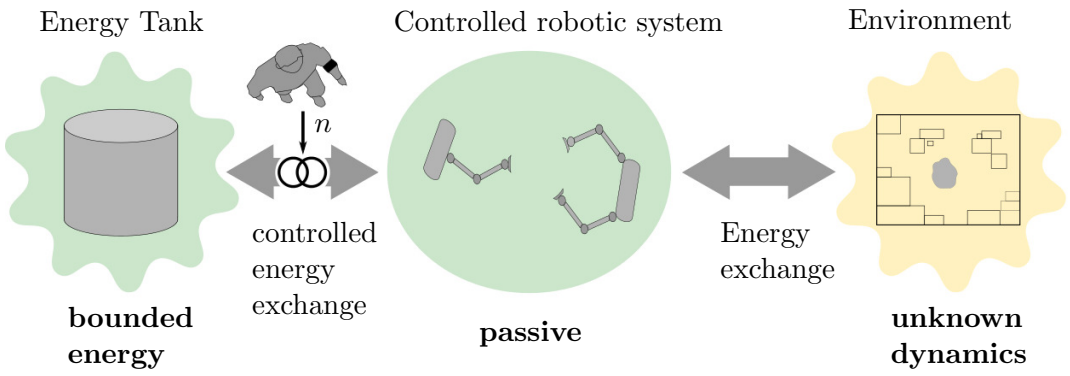

Figure 3.2: The human operator controls the energy flow between tank and robotic system

3.2 Energy tanks

The motivation for the use of an *energy tank* is to energetically decouple the human operator from the robotic system, i.e. the operator is no longer able to supply energy to the system. This is a consequence of the chosen input method, which is based on information rather than on energy exchange, as discussed above. The energy necessary for driving the robotic system comes from the tank, the operator only controls the energetic flow. The scheme is illustrated in figure 3.2.

On command of the operator energy flows from the energy tank into the controller and on into the robotic system. Under ideal conditions energy is circulating between these parts and the total amount stays constant (lossless system). In subsection 3.2.2 cases of a permanent change of the energy balance are discussed. At first the combination of an energy tank and one of the controllers proposed in section 2.6, is analysed. Thereby no energy exchange with the robotic system is assumed. In this case a lossless combined system is guaranteed by re-harvesting the energy dissipated in the controller's dampers. Re-harvesting means that the energy, that is only virtually dissipated in the controller, becomes available again by supplying it back into the tank.
The energy tank is a virtual storage element defined with a Hamiltonian energy function. Let $x_\mathrm{t} \in \mathbb{R}$ denote the (scalar) energy state and $\mathcal{T}$ be a simple, positive definite function $\mathcal{T}(x_\mathrm{t}) = \frac{1}{2}x_\mathrm{t}^2$. The dynamic equations of the tank are

$$\begin{aligned} \dot{x_\mathrm{t}} &= f_\mathrm{t} \\ e_\mathrm{t} &= \frac{\partial \mathcal{T}(x_\mathrm{t})}{\partial x_\mathrm{t}} (= x_\mathrm{t}) \end{aligned} \tag{3.2}$$

Here $(f_\mathrm{t}, e_\mathrm{t})$ is the flow-effort pair, corresponding to input and output respectively. The application of the energy tank is demonstrated with an example port-Hamiltonian system of the standard input-state-output form, given in equation 2.11. This stan-

dard system is chosen to keep the derivation process simple and can be replaced with the controllers from section 2.6. The re-routing of the virtually dissipated energy into the tank is accomplished by choosing the tank input as

$$f_\mathrm{t} = \frac{1}{x_\mathrm{t}} \frac{\partial^T \mathcal{H}}{\partial \boldsymbol{x}} D(\boldsymbol{x}) \frac{\partial \mathcal{H}}{\partial \boldsymbol{x}} + \tilde{f}_\mathrm{t} \tag{3.3}$$

The term $\frac{\partial^T \mathcal{H}}{\partial \boldsymbol{x}} D(\boldsymbol{x}) \frac{\partial \mathcal{H}}{\partial \boldsymbol{x}}$ is the dissipated power. A new input $\tilde{f}_\mathrm{t}$ is defined to preserve the power port for interconnection with the controller. With the new input the tank's energy balance becomes

$$\dot{\mathcal{T}}(x_\mathrm{t}) = e_\mathrm{t} f_\mathrm{t} = \frac{\partial^T \mathcal{H}}{\partial \boldsymbol{x}} D(\boldsymbol{x}) \frac{\partial \mathcal{H}}{\partial \boldsymbol{x}} + x_\mathrm{t} \tilde{f}_\mathrm{t} \tag{3.4}$$

This corresponds to the systems dissipated energy plus some external supply. Next this external supply is used to interconnect tank and the standard port-Hamiltonian system, representing the controller. A power-preserving interconnection is established, which is a combination of gyrator and transformer with ratio $\boldsymbol{n}$. This type of interconnection allows the operator to control the power flow, despite being energetically decoupled.

$$\begin{aligned} \boldsymbol{u} &= \boldsymbol{n} e_\mathrm{t} \\ \tilde{f}_\mathrm{t} &= -\boldsymbol{n}^T \boldsymbol{y} \end{aligned} \tag{3.5}$$

By construction and independent of a particular choice of $\boldsymbol{n}$ this relation is power-continuous

$$\boldsymbol{u}^T \boldsymbol{y} = e_\mathrm{t}^T \boldsymbol{n}^T \boldsymbol{y} = -e_\mathrm{t}^T \tilde{f}_\mathrm{t} \tag{3.6}$$

i.e. the transformer/gyrator is lossless for any $\boldsymbol{n}$. The choice of $\boldsymbol{n}$ is not fixed but can be adjusted dynamically to shape the energy flow. In particular it is appealing to use $\boldsymbol{n}$ to replicate the original control signal by choosing $\boldsymbol{n} = \frac{\boldsymbol{w}}{x_\mathrm{t}}$. The new control input $\boldsymbol{w}$ can effectively take the role of $\boldsymbol{u}$, i.e. the port-Hamiltonian system becomes

$$\dot{\boldsymbol{x}} = [J(\boldsymbol{x}) - D(\boldsymbol{x})] \frac{\partial \bar{\mathcal{H}}}{\partial \boldsymbol{x}} + G(\boldsymbol{x}) \frac{\boldsymbol{w}}{x_\mathrm{t}} e_\mathrm{t} = [J(\boldsymbol{x}) - D(\boldsymbol{x})] \frac{\partial \bar{\mathcal{H}}}{\partial \boldsymbol{x}} + G(\boldsymbol{x}) \boldsymbol{w} \tag{3.7}$$

The combined Hamiltonian energy function of the interconnected system is $\bar{\mathcal{H}}(\boldsymbol{x}, x_\mathrm{t}) = \mathcal{H}(\boldsymbol{x}) + \mathcal{T}(x_\mathrm{t})$. An empty energy tank, i.e. $x_t = 0$, results in a division by zero in equation (3.7). Thus an complete depletion of the tank must be avoided. A minimum strategy is to introduce a switching parameter α. The transformer ratio is extended to $\boldsymbol{n} = \frac{\alpha \boldsymbol{w}}{x_\mathrm{t}}$ with

$$\alpha = \begin{cases} 1 & \text{if } \mathcal{T}(x_\mathrm{t}) \geq \epsilon > 0 \\ 0 & \text{if } \mathcal{T}(x_\mathrm{t}) < \epsilon \end{cases} \tag{3.8}$$

This means that a control input is executed unchanged as long as certain amount ϵ of energy is in the tank. Once the tank is almost empty, i.e. $\mathcal{T}(x_\mathrm{t}) < \epsilon$, further command execution possibly violates passivity. A negative energy level of the (virtual) tank has no physical meaning and compromises passivity by generating energy. The switching parameter α sets the input to 0, thus effectively suspending energy exchange. This happens in both ways, neither is it possibly to re-transfer energy into the tank through the interconnection. At this point the tank can only be refilled by dissipation. Dissipation is associated with kinetic energy, i.e. as long as the system is moving it can recover from the input-suspended state. If the system is driven to a state of exclusively potential energy, there is no dissipation to refill the tank. If the tank is emptied below the threshold level, the input is ultimately suspended. The system cannot recover anymore because there is no kinetic energy to be dissipated and the switching parameter prevents the energy exchange with the controller.
The controllers designed in section 2.6 store potential energy for two reasons, one is due to gravitation, the other is for deviations of desired and actual position. Gravitation is the more unproblematic case, elevating the system means to move the system. Moving means dissipating energy. In the elevating process a snmall portion of energy is dissipated and re-supplied to the tank. When getting close to the tank threshold, the available energy to be transformed into kinetic and then into potential energy gets asymptotically smaller. Only the previously dissipated energy is available and the elevation slows down and approaches to zero speed. Thus reaching a state of exclusively gravitational potential energy takes infinite time. Deviations of actual and desired position result in potential energy stored in the springs connecting operator-object and object-manipulators. Consider now the system driven into an obstacle and the operator persisting to command motion in the blocked direction. The operator sets the desired object position and thus the springs are elongated. There is no dissipation because the system is blocked. If the dislocation consumes all the available energy, the system is deadlocked, i.e. the systems inputs are suspended permanently.
Another apparent issue with the binary parameter α is the abrupt switching behaviour if the tank level is in the neighbourhood of ϵ. Numeric simulations indicate high forces and chattering behaviour.
A solution to this desired behaviour is to make α a function of the tank level and continuously scale the desired trajectory.

$$\alpha = \begin{cases} 1 & \text{if } \mathcal{T}(x_\mathrm{t}) \geq \mathcal{T}_{th} \\ \frac{\mathcal{T}(x_\mathrm{t})-\epsilon}{\mathcal{T}_\mathrm{th}} & \text{if } \epsilon \leq \mathcal{T}(x_\mathrm{t}) < \mathcal{T}_\mathrm{th} \\ 0 & \mathcal{T}(x_\mathrm{t}) < \epsilon \end{cases} \tag{3.9}$$

where $\mathcal{T}_\mathrm{th} > \epsilon$ is a threshold level that defines the width of the transition region. Adapting the reference trajectory leads to a permanent position deviation, if the user does not actively readjust after the tank level has recovered. The next subsection addresses this problem.

Regardless of a particular choice of α, a combined port-Hamiltonian representation of the system and the tank is as follows

$$\begin{pmatrix} \dot{\boldsymbol{x}} \\ \dot{x}_\mathrm{t} \end{pmatrix} = \left[\begin{pmatrix} J(\boldsymbol{x}) & \frac{\alpha \boldsymbol{w}}{x_\mathrm{t}} \\ -\frac{\alpha \boldsymbol{w}^T}{x_\mathrm{t}} & 0 \end{pmatrix} - \begin{pmatrix} D(\boldsymbol{x}) & 0 \\ -\frac{1}{x_\mathrm{t}} \frac{\partial^T \bar{\mathcal{H}}}{\partial \boldsymbol{x}} D(\boldsymbol{x}) & 0 \end{pmatrix} \right] \begin{pmatrix} \frac{\partial \bar{\mathcal{H}}}{\partial \boldsymbol{x}} \\ \frac{\partial \bar{\mathcal{H}}}{\partial x_\mathrm{t}} \end{pmatrix} \tag{3.10}$$

Note that there is no more an input-output port. This is because the external ports are defined by energy exchange of the system with its environment. It is shown in subsection 2.2.1 that systems, consistent with (2.11), are passive. Analogously the described combination of such a system and the energy tank is *lossless*:

$$\begin{aligned} &\frac{d}{dt}\bar{\mathcal{H}}(\boldsymbol{x}, x_\mathrm{t}) = \begin{pmatrix} \frac{\partial^T \bar{\mathcal{H}}}{\partial \boldsymbol{x}} & \frac{\partial^T \bar{\mathcal{H}}}{\partial x_\mathrm{t}} \end{pmatrix} \begin{pmatrix} \dot{\boldsymbol{x}} \\ \dot{x}_\mathrm{t} \end{pmatrix} = \frac{\partial^T \bar{\mathcal{H}}}{\partial \boldsymbol{x}} J(\boldsymbol{x}) \frac{\partial \bar{\mathcal{H}}}{\partial \boldsymbol{x}} + \frac{\partial^T \bar{\mathcal{H}}}{\partial \boldsymbol{x}} \frac{\alpha \boldsymbol{w}}{x_\mathrm{t}} \frac{\partial \bar{\mathcal{H}}}{\partial x_\mathrm{t}} \\ &- \frac{\partial^T \bar{\mathcal{H}}}{\partial \boldsymbol{x}} D(\boldsymbol{x}) \frac{\partial \bar{\mathcal{H}}}{\partial \boldsymbol{x}} - \frac{\partial^T \bar{\mathcal{H}}}{\partial x_\mathrm{t}} \frac{\alpha \boldsymbol{w}^T}{x_\mathrm{t}} \frac{\partial \bar{\mathcal{H}}}{\partial \boldsymbol{x}} + \frac{\partial^T \bar{\mathcal{H}}}{\partial x_\mathrm{t}} \frac{1}{x_\mathrm{t}} \frac{\partial^T \bar{\mathcal{H}}}{\partial \boldsymbol{x}} D(\boldsymbol{x}) \frac{\partial \bar{\mathcal{H}}}{\partial \boldsymbol{x}} = 0 \end{aligned} \tag{3.11}$$

3.2.1 Energy-adapted stiffness and damping

With the above conjunction of tank and controller control inputs are discarded, as soon as the energy tank is depleted. It is clear that desired trajectories driving the tank to a negative state are not feasible with the given energy budget and need to be altered. Simply discarding the desired trajectory information leads to a permanent deviation of the position. Optimal trajectory following demands a controller that returns the system onto the desired trajectory, as soon as the energy level has recovered.

Therefore the proposal is to use an energy-adapted spring and damper. The idea is to relax the stiffness of the user-object spring as function of the available energy. Actually the impedance of the human hand behaves similar, usually it is stiff for slow motion and compliant during fast movements (high kinetic energy, likely depleted energy tank) [Hog84a]. A lower stiffness allows the system to "float" loosely, while the tank gets re-filled through the damping.

Moreover a change of stiffness affects the energy stored in the spring, relaxing stiffness sets energy free, which is re-supplied into the tank. With a rise of the tank level, stiffness is increased and the spring re-directs the system onto the desired trajectory. The illustration of the principle starts with an example one-dimensional spring given by

$$F = k_{vb}(x_v - x_b) \ , \ \mathcal{T}(x_\mathrm{t}) \geq \mathcal{T}_\mathrm{th} \tag{3.12}$$

This equation is valid if the tank level $\mathcal{T}(x_\mathrm{t})$ is above a certain threshold level $\mathcal{T}_\mathrm{th}$. The stiffness of the spring $k_{vb} \in \mathbb{R}^+$ is constant, $x_v, x_b \in \mathbb{R}$ denote the reference and the actual position respectively. Below the threshold the following spring function is proposed

$$F = k_{vb} \frac{\mathcal{T}(x_\mathrm{t})}{\mathcal{T}_\mathrm{th}} (x_v - x_b) \ , \ \mathcal{T}(x_\mathrm{t}) < \mathcal{T}_\mathrm{th} \tag{3.13}$$

For ease of notation a new stiffness parameter is introduced

$$\kappa = \begin{cases} k_{vb} & \text{if } \mathcal{T}(x_\mathrm{t}) \geq \mathcal{T}_\mathrm{th} \\ k_{vb}\frac{\mathcal{T}(x_\mathrm{t})}{\mathcal{T}_\mathrm{th}} & \text{if } \mathcal{T}(x_\mathrm{t}) < \mathcal{T}_\mathrm{th} \end{cases} \tag{3.14}$$

The corresponding energy function is then

$$V_\kappa(x_v, x_b, \kappa) = \frac{1}{2}\kappa(x_v - x_b)^2 \tag{3.15}$$

The exchanged power with respect to a change of stiffness is

$$\dot{V}_\kappa = \frac{\partial V_\kappa}{\partial \kappa}\frac{d\kappa}{dt} = \frac{1}{2}(x_v - x_b)^2\dot{\kappa} = e_\mathrm{k}^T f_\mathrm{k}, \tag{3.16}$$

which corresponds to the product of effort ($\frac{\partial V_\kappa}{\partial \kappa}$) and flow ($\dot{\kappa}$) and forms a power port ($f_\mathrm{k}, e_\mathrm{k}$) as defined in Section 2.2. The energy function of a 6-DoF spring is of the from

$$V_\kappa : SE(3) \times \mathcal{K} \to \mathbb{R}; (H_b^v, \kappa) \mapsto V_\kappa(H_b^v, \kappa), \tag{3.17}$$

which is equal to the previous spring energy function (eq. (2.40)) but depends explicitly on the stiffness parameter κ. $\mathcal{K}$ is a parametric space that equals $\mathbb{R}$ in case of an isotropic spring. For more information on variable spatial springs see [SD01]. The port-Hamiltonian representation of a variable stiffness spring is given by

$$\begin{aligned} \begin{pmatrix} \dot{H}_b^v \\ \dot{\kappa} \end{pmatrix} &= \begin{pmatrix} H_b^v & 0 \\ 0 & I \end{pmatrix} \begin{pmatrix} T_b^{b,v} \\ f_\mathrm{k} \end{pmatrix} \\ \begin{pmatrix} W_b^{b,v} \\ e_\mathrm{k} \end{pmatrix} &= \begin{pmatrix} H_b^{vT} & 0 \\ 0 & I \end{pmatrix} \begin{pmatrix} \frac{\partial V_\kappa}{\partial H_b^v} \\ \frac{\partial V_\kappa}{\partial \kappa} \end{pmatrix}, \end{aligned} \tag{3.18}$$

where $f_\mathrm{k}, e_\mathrm{k}$ is the input-output pair. Towards pairing the variable stiffness spring with the energy tank one can express κ as a function of the tank level. Using the tank power flow equation (3.4) leads

$$\dot{\kappa} = \begin{cases} 0 & \text{if } \mathcal{T}(x_\mathrm{t}) \geq \mathcal{T}_\mathrm{th} \\ \frac{k}{\mathcal{T}_\mathrm{th}}\dot{\mathcal{T}}(x_\mathrm{t}) = \frac{k_{vb}}{T_\mathrm{th}}\dot{x}_\mathrm{t}\frac{\partial \bar{\mathcal{H}}}{\partial x_\mathrm{t}} & \text{if } \mathcal{T}(x_\mathrm{t}) < \mathcal{T}_\mathrm{th} \end{cases} \tag{3.19}$$

The power exchanged between variable spring and tank due to stiffness changes is

$$\dot{\bar{\mathcal{H}}} = \frac{\partial \bar{\mathcal{H}}}{\partial \kappa}\dot{\kappa} = \begin{cases} 0 & \text{if } \mathcal{T}(x_\mathrm{t}) \geq \mathcal{T}_\mathrm{th} \\ \frac{\partial \bar{\mathcal{H}}}{\partial \kappa}\frac{k_{vb}}{\mathcal{T}_{th}}\dot{x}_\mathrm{t}\frac{\partial \bar{\mathcal{H}}}{\partial x_\mathrm{t}} & \text{if } \mathcal{T}(x_\mathrm{t}) < \mathcal{T}_\mathrm{th} \end{cases} \tag{3.20}$$

The power exchanged by the energy tank is of the form $\dot{\mathcal{T}}(x_\mathrm{t}) = \frac{\bar{\mathcal{H}}}{\partial x_\mathrm{t}} f_\mathrm{t}$, therefore $\frac{\partial \bar{\mathcal{H}}}{\partial \kappa}\frac{k_{vb}}{\mathcal{T}_\mathrm{th}}\dot{x}_\mathrm{t}$ is an input for the energy tank. Using these assignments one obtains the

port-Hamiltonian representation of variable stiffness spring and energy tank. For simplicity, here the variable stiffness spring is part of the general system of equation (2.11)

$$\begin{pmatrix} \dot{\boldsymbol{x}} \\ \dot{x}_\mathrm{t} \\ \dot{\kappa} \end{pmatrix} = \left[\begin{pmatrix} J(\boldsymbol{x}) & \frac{\alpha \boldsymbol{w}}{x_\mathrm{t}} & 0 \\ -\frac{\alpha \boldsymbol{w}^T}{x_\mathrm{t}} & 0 & -\frac{k_{vb}}{\mathcal{T}_\mathrm{th}} \dot{x}_\mathrm{t} \\ 0 & \frac{k_{vb}}{\mathcal{T}_\mathrm{th}} \dot{x}_\mathrm{t} & 0 \end{pmatrix} - \begin{pmatrix} D(\boldsymbol{x}) & 0 & 0 \\ -\frac{1}{x_\mathrm{t}} \frac{\partial \bar{\mathcal{H}}^T}{\partial \boldsymbol{x}} D(\boldsymbol{x}) & 0 & 0 \\ 0 & 0 & 0 \end{pmatrix} \right] \begin{pmatrix} \frac{\partial \bar{\mathcal{H}}}{\partial \boldsymbol{x}} \\ \frac{\partial \bar{\mathcal{H}}}{\partial x_\mathrm{t}} \\ \frac{\partial \bar{\mathcal{H}}}{\partial \kappa} \end{pmatrix} \tag{3.21}$$

The combination of such an example system with a variable stiffness spring and a tank is lossless, disregarding the energy exchange with the robotic environment.

$$\begin{aligned} \frac{d}{dt} \bar{\mathcal{H}}(\boldsymbol{x}, x_\mathrm{t}, \kappa) &= \begin{pmatrix} \frac{\partial^T \bar{\mathcal{H}}}{\partial \boldsymbol{x}} & \frac{\partial^T \bar{\mathcal{H}}}{\partial x_\mathrm{t}} & \frac{\partial^T \bar{\mathcal{H}}}{\partial \kappa} \end{pmatrix} \begin{pmatrix} \dot{\boldsymbol{x}} \\ \dot{x}_\mathrm{t} \\ \dot{\kappa} \end{pmatrix} = \frac{\partial^T \bar{\mathcal{H}}}{\partial \boldsymbol{x}} J(\boldsymbol{x}) \frac{\partial \bar{\mathcal{H}}}{\partial \boldsymbol{x}} + \frac{\partial^T \bar{\mathcal{H}}}{\partial \boldsymbol{x}} \frac{\alpha \boldsymbol{w}}{x_\mathrm{t}} \frac{\partial \bar{\mathcal{H}}}{\partial x_\mathrm{t}} \\ &- \frac{\partial^T \bar{\mathcal{H}}}{\partial \boldsymbol{x}} D(\boldsymbol{x}) \frac{\partial \bar{\mathcal{H}}}{\partial \boldsymbol{x}} - \frac{\partial^T \bar{\mathcal{H}}}{\partial x_\mathrm{t}} \frac{\alpha \boldsymbol{w}^T}{x_\mathrm{t}} \frac{\partial \bar{\mathcal{H}}}{\partial \boldsymbol{x}} - \frac{\partial^T \bar{\mathcal{H}}}{\partial x_\mathrm{t}} \frac{k_{vb}}{T_\mathrm{th}} \dot{x}_\mathrm{t} \frac{\partial \bar{\mathcal{H}}}{\partial \kappa} + \frac{\partial^T \bar{\mathcal{H}}}{\partial x_\mathrm{t}} \frac{1}{x_\mathrm{t}} \frac{\partial^T \bar{\mathcal{H}}}{\partial \boldsymbol{x}} D(\boldsymbol{x}) \frac{\partial \bar{\mathcal{H}}}{\partial \boldsymbol{x}} \\ &+ \frac{\partial^T \bar{\mathcal{H}}}{\partial \kappa} \frac{k_{vb}}{T_\mathrm{th}} \dot{x}_\mathrm{t} \frac{\partial \bar{\mathcal{H}}}{\partial x_\mathrm{t}} = 0 \end{aligned} \tag{3.22}$$

The dissipative structure $D(\boldsymbol{x})$ can be changed without compromising passivity as long as it is positive semi-definite. A change of a damping parameter does not change the energy stored in the system, since dampers do not store energy and do not have a state variable. A similar approach as for stiffness indicates good results in numeric simulations. With a depletion of the energy tank the damping $d_{vb} \in \mathbb{R}^+$ along the user-object spring is reduced, thus the coupling between user and virtual object is further relaxed.

$$\delta = \begin{cases} d_{vb} & \text{if } \mathcal{T}(x_\mathrm{t}) \geq \mathcal{T}_\mathrm{th} \\ d_{vb} \frac{\mathcal{T}(x_\mathrm{t})}{\mathcal{T}_{th}} & \text{if } \mathcal{T}(x_\mathrm{t}) < \mathcal{T}_\mathrm{th} \end{cases} \tag{3.23}$$

3.2.2 Energy exchange with the robotic system and environment

So far, there was the simplification of assuming no energy exchange of the controller through the robots with the environment. In contrast to the human-controller relation, the controller-robot relation is established on an energetic level. The robot measures its velocity at exactly the same point it applies the commanded force. This defines the power port between the controller and the robotic environment. The power flow through this port can affect the energy of the tank-controller permanently, i.e. an irreversible drain of energy is possible. In the following three important cases are discussed that interfere with the concept of a constant energy level in tank and controller.

In the controllers of section 2.6 the robots are a simple inertias. In reality however

they are a system of actuated joints and links with a dynamic behaviour different from a single inertia. To achieve the desired control performance the robots can be pre-compensated by passive feedback-linearisation [OASK+04]. The internal dynamics and gravity are compensated in favour of shaping a desired inertia. This technique however is passive, but not lossless, because lossless would require ideal measurements and modelling. This means, at this point energy is irreversibly dissipated.
The second issue is the friction in the robot's joints, it can degrade precision and results in a loss of energy seen from the controller-robot power port. In [TASLH08] a passive observer/compensation technique is presented that estimates the torque necessary to overcome friction and applies it in addition. Although this method reduces the energy loss due to friction, it is still a cautious estimation (i.e. passive) and not lossless. Thus, over time the energy stored in robots, controller and energy tank decreases.
A permanent drain of energy in the system occurs, if the robotic system is performing work on the environment. For example, let the common object (connected to the robots) move other objects in the workspace. The work performed on this objects is withdrawn permanently from the energy balance.
Clearly, there is always a drain of energy in a realistic system and at some time the energy tank gets close to depletion. In this case energy has to be supplied to the system, in order to restore the capacity to act. It is clear that this means the introduction of a source of energy and thus inflicts a loss of the strict definition of passivity. The safest way of re-powering the system is to allow the operator to supply energy to the tank, in a manner independent of the motion control interface. This means the operator is always in charge of the energy content and is able to estimate the possible impact on the environment. However the approach may be inconvenient, in certain operations the user has to interrupt his actual work and choose an appropriate quantum of energy to send to the energy tank. This may mislead some operators to use higher quanta than those indicated by the safety metrics in section 3.1. Clearly this makes the concept of safety by limited energy ineffective. Therefore an automatic strategy to compensate for energy drain is discussed in the next subsection.
With no restrictive assumptions on the environment, energy supply by the environment have to be considered. For safety reasons it is advisable to automatically discard energy supplied to the tank that exceeds the initial level.

Automatic compensation for drained energy

The two controllers presented in section 2.6 are based on the model of a cooperative manipulation set-up. In an ideal case the same amount of energy stored in the energy is virtually bound in the controller, i.e. the controller reflects the energy state of the real system. Since all energy sourced by the tank flows through the controller into the robots, bounding the energy in the controller also limits the energy stored

in the robotic system. It is thus sufficient to apply the energetic limits, imposed by the safety metrics, to the controller. The proposed automatic compensation re-supplies the energy transferred to the robots into the energy tank. The power exchanged between controller and the i-th robot is defined by the wrench-twist product $(W_i^{0,0})^T T_i^0$, applying the automatic compensation the energy balance is

$$\dot{\mathcal{T}}(x_\mathrm{t}) + \underbrace{\sum_{i=1}^{n} (W_i^{0,0})^T T_i^0}_{\text{compensation}} = -\dot{\mathcal{H}}(x) + \sum_{i=1}^{n} (W_i^{0,0})^T T_i^0 \tag{3.24}$$

This means a constant level of energy in tank and controller $\dot{\mathcal{T}}(x_\mathrm{t}) + \dot{\mathcal{H}} = 0$. Clearly, the compensation term $\sum_{i=1}^{n} (W_i^{0,0})^T T_i^0$ is active. It provides energy in lieu of the user, who is energetically decoupled in our approach. Still all energy flows through the controller and is bounded if necessary. But the energy budget, given by the tank level, accounts only for the controller state. Please recall that the combination of controller and tank is lossless, so the system can always carry out tasks within the given safety margin.

In order to explain the proposal of enhancing stability and safety by energy-bounding the controller, consider the following illustrative examples. The operator drives the system to a high velocity, due to the moving virtual inertias in the controller, the tank is used up. This leads to a relaxation of the coupling of user and virtual object and prevents further acceleration. Thus the robotic system is kept at a certain speed. This also holds if the virtual inertia parameters deviate from their real pendants (modelling errors). The combination of the initial tank level and the virtual inertias determine the achievable system speed. It is possible to calculate this speed by using the apparent inertia of a cooperative set-up from [EH16].

Please consider again the introductory case of robots driven into an obstacle and a user still to command motion in the blocked direction. The user-object spring is elongated and its potential energy empties the tank. The automatic compensation provides no energy to the tank, because the robots are blocked and do not move, i.e. no power is exchanged. With the depletion of the tank, stiffness and damping of the user spring are reduced. This keeps the forces bounded even if the user does not change her/his commands. Conclusively the total wrench that the common object can exert on the environment is determined by the initial tank level and the spring stiffness.

Chapter 4

Simulation results

Simulations of the proposed control schemes and existing approaches from literature are conducted to evaluate and compare their effectiveness. The controllers for cooperative manipulation are compared in terms of trajectory tracking and internal stress on the object. To preserve comparability, they are adjusted to exert equal force and the tuning parameters are kept within the same range.
In the simulation the robots are assumed to behave like simple inertias, i.e. their underlying dynamics (configuration dependent inertia, Coriolis and gravity terms) is compensated. The connection between common object (another inertia) and the end-effectors is considered rigid. For the computation of the combined dynamics the principle of least constraint motion is applied, which is explicitly given for a cooperative manipulation set-up in [EH16]. The same article provides the routine used for the calculation of the stress exerted on the object (internal wrench). Simulations are conducted in *MATLAB/Simulink*, using a fixed step solver with a step size of 1ms. This facilitates application in an experimental set-up (the control units typically run at 1kHz). The Parameters used in the simulations can be found in table 4.1. The control input is a reference velocity, the set-point position/orientation is computed by integration. Fig. 4.1 shows the two test cases, linear (along the x-axis) and angular velocity (around the z-axis).

Table 4.1: General simulation settings

Number of manipulators	4
Object inertia M_b	1.4 kg $\cdot I_3$ (lin.), 0.2 kgm^2 $\cdot I_3$ (ang.)
Manipulator inertia M_i	10 kg $\cdot I_3$ (lin.), 0.5 kgm^2 $\cdot I_3$ (ang.)
Object diameter	0.8m

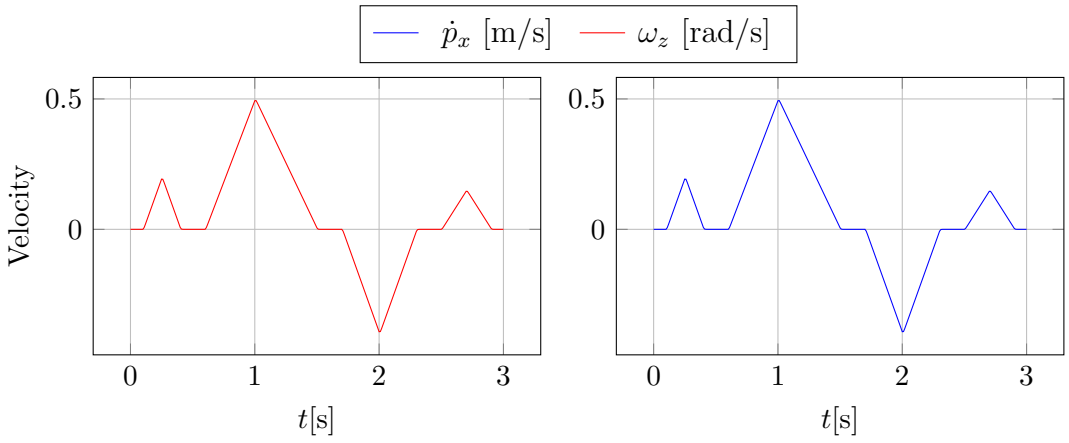

Figure 4.1: Test reference trajectories for translation (left) and rotation

4.1 State-of-the-art control schemes for cooperative manipulation

In literature several control schemes for cooperative manipulation are known. The focus is limited to those that achieve stability during contact and non-contact transitions. Those include impedance control and Intrinsically Passive Control (IPC). Simulation results are provided for two impedance control schemes and one IPC scheme. The dynamic performance is discussed with regard to the different role of inertias in either control paradigms.

4.1.1 Internal and external impedance based reference trajectory generation

A renowned approach by Caccavale and Villani [CV01, CCMV08] consists of a cascaded architecture enforcing two impedance relations. One is established between the given reference trajectory and the object, termed as the *external* impedance. The other is between the manipulators and the object and is called the *internal* impedance. The output of the impedance loops is a compliant reference trajectory which is used in an *inner motion control* loop to generate forces to drive the robot. The parameters used in the simulation are chosen very close to the ones given in [CCMV08], see table 4.2.
The simulation results are presented in figure 4.2, the left column shows the linear motion test case and the right the rotational one. The plots on top show the deviation from the desired position and orientation respectively. The velocity errors are displayed below. The third plot row shows the wrenches applied by one of the manipulators. The bottom row indicates the internal stress a manipulator exerts on the object.
The approach shows good trajectory tracking. The velocity error is the lowest in

this comparative study. The internal wrench is low and is similar to the other approaches. For pure linear motion the internal stress is approx. zero.

4.1.2 Internal impedance control with feed-forward of the object dynamics

Erhart and Hirche [EH16] omit the external impedance relation, but include object dynamics feed-forward, i.e. the wrench necessary to accelerate the object's inertia is distributed by an inverse of the grasp matrix to the manipulators. This results in even better position/orientation accuracy compared to the approach presented in subsection 4.1.1. However results presented in [CCMV08] indicate that, in absence of an external impedance relation, higher forces occur, if the object comes into contact with the environment.
Interestingly the magnitude of the internal forces (during rotation) depends directly on the step size of the simulation (running a fixed step solver), i.e. a ten-times smaller step size gives ten-times smaller internal forces. Internal forces are calculated based on the geometry in the last simulation step. The correlation between step size and values indicates that these forces are rather a consequence of the discrete nature of the simulation than of the control law generating internal stress.
Table 4.3 shows the parameters used and the results can be seen from figure 4.3.

4.1.3 Dynamic IPC

The IPC is introduced by Stramigioli [Str01b] and experimentally evaluated by Wimböck et al. [WOH08] on a robotic hand. Stramigioli applies pure stiffness control, i.e. there are no dampers along the springs. Wimböck et al. add the dampers to enhance the trajectory tracking behaviour and call the scheme *dynamic IPC*. See also figure 4.4 for a comparison. The implementation of Wimböck is purely translational, i.e. forces but no moments are transferred via the springs and the dampers. The simulation results presented here, called dynamic IPC, are a combination of both approaches, dampers along the 6-DoF springs are used.
The impedance parameters are chosen equal or lower for translation and significantly

Table 4.2: Parameters for dual impedance controlled reference trajectory generation

	linear	angular
Ext. inertia	$0.7\text{kg} \cdot I_3$	$0.1\text{kgm}^2 \cdot I_3$
Ext. damping	$1500\text{kg/s} \cdot I_3$	$10\text{kgm}^2/\text{s} \cdot I_3$
Ext. stiffness	$700\text{N/m} \cdot I_3$	$5\text{Nm} \cdot I_3$
Int. inertia	$10\text{kg} \cdot I_3$	$0.5\text{kgm}^2 \cdot I_3$
Int. damping	$1000\text{kg/s} \cdot I_3$	$80\text{kgm}^2/\text{s} \cdot I_3$
Int. stiffness	$400\text{N/m} \cdot I_3$	$2\text{Nm} \cdot I_3$

Table 4.3: Parameters for the internal impedance control with object dynamics feed-forward

	linear	angular
Object inertia ff.	$1.4\text{kg} \cdot I_3$	$0.2\text{kgm}^2 \cdot I_3$
Int. inertia	$10\text{kg} \cdot I_3$	$0.5\text{kgm}^2 \cdot I_3$
Int. damping	$1000\text{kg/s} \cdot I_3$	$80\text{kgm}^2/\text{s} \cdot I_3$
Int. stiffness	$400\text{N/m} \cdot I_3$	$2\text{Nm} \cdot I_3$

higher for rotation, see table 4.4.
The feasible stiffness and damping in this implementation is limited by numerical stability, a further increase leads to infinite values at some point of the simulation. This issue also requires the use of *Simulink's ode8* solver for this approach, instead of *ode1* (Euler's method) used for the other simulations. The *ode8* method is of the *Dormand-Prince* class with an accuracy order of 8. The rate of rate of convergence improves at the cost of higher computational complexity [Mat16].
The results (fig. 4.5) show a clearly inferior trajectory tracking compared to the previous approaches.

Discussion

The difference of dynamic performance of impedance control and IPC stems from a different mode of function of the inertias in the IPC. In classic impedance control clearly the inertia is in parallel with the spring and in the IPC the inertia is connected in series, figure 4.4 illustrates the concepts. In the first case the inertia is used to calculate the wrench necessary to accelerate the associated body, in the latter the spring (and damper) need to provide the wrench to accelerate the additional (virtual) body. Thus the inertia in the IPC is an energy storing element that reduces the controller dynamics. On the other hand the IPC does not require absolutely smooth reference velocities. The classic impedance control approaches use the time-derivative of the input velocity and often require pretreatment (e.g. low-pass filtering) of the input.

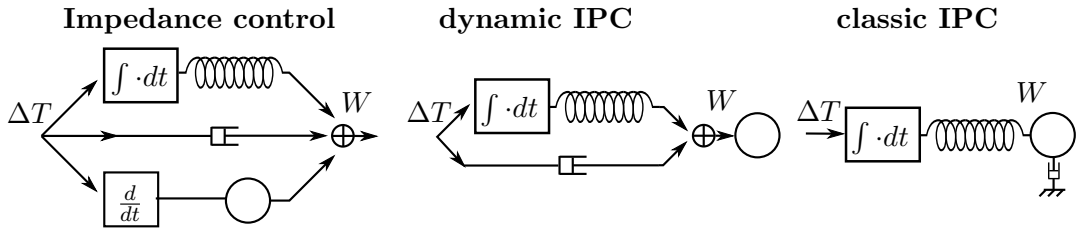

Figure 4.4: Arrangement of spring, mass and damper in classical impedance control, dynamic [WOH08] and classic IPC [Str01b]

Table 4.4: Parameters for the IPC

	linear	angular
Virt. inertia	$1.4\text{kg} \cdot I_3$	$0.2\text{kgm}^2 \cdot I_3$
Ext. damping	$1500\text{kg/s} \cdot I_3$	$500\text{kgm}^2/\text{s} \cdot I_3$
Ext. stiffness	$700\text{N/m} \cdot I_3$	$400\text{Nm} \cdot I_3$
Int. damping	$625\text{kg/s} \cdot I_3$	$31.25\text{kgm}^2/\text{s} \cdot I_3$
Int. stiffness	$125\text{N/m} \cdot I_3$	$6.25\text{Nm} \cdot I_3$

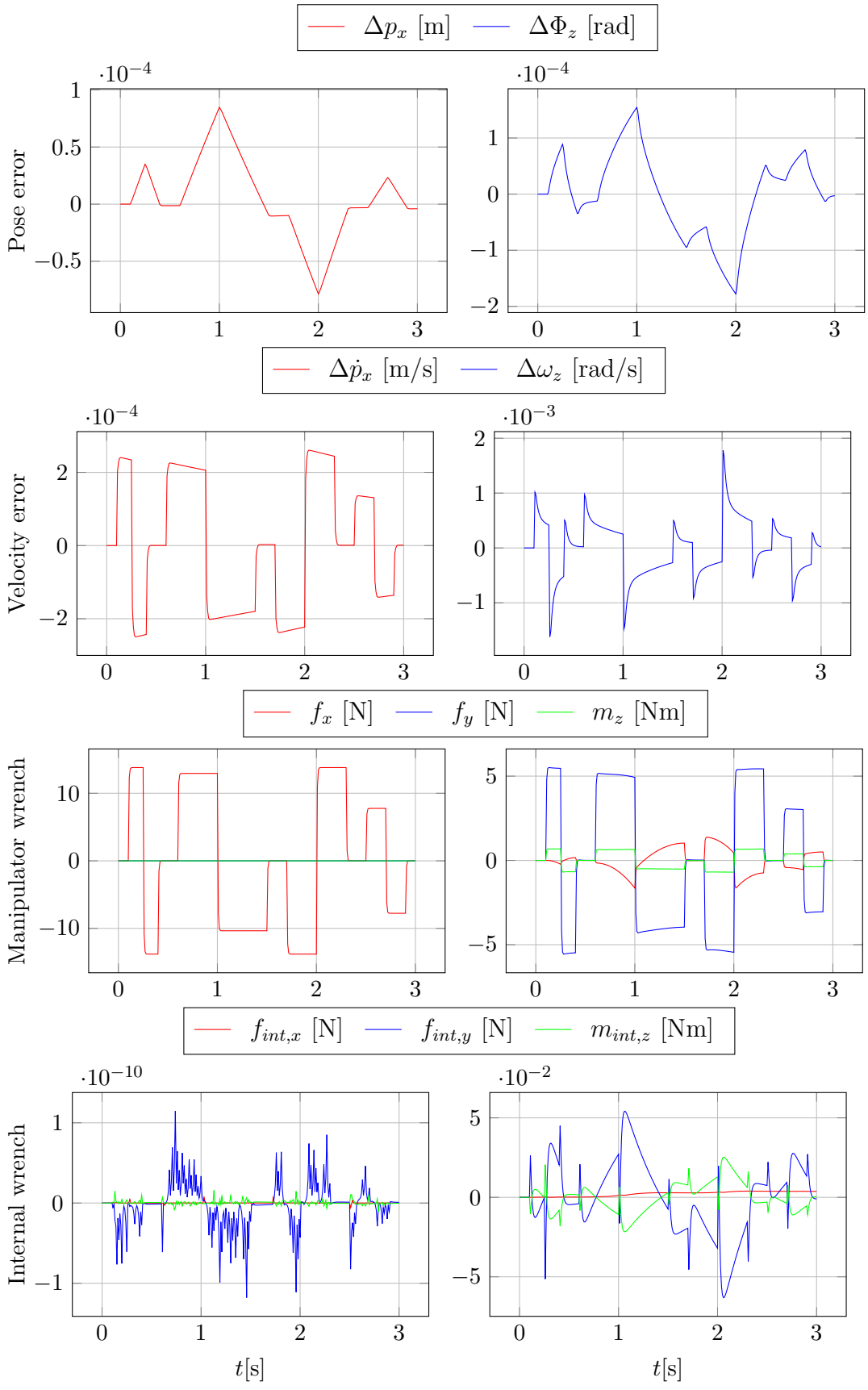

Figure 4.2: Internal and external impedance based reference trajectory generation: Translation (left column) and rotation

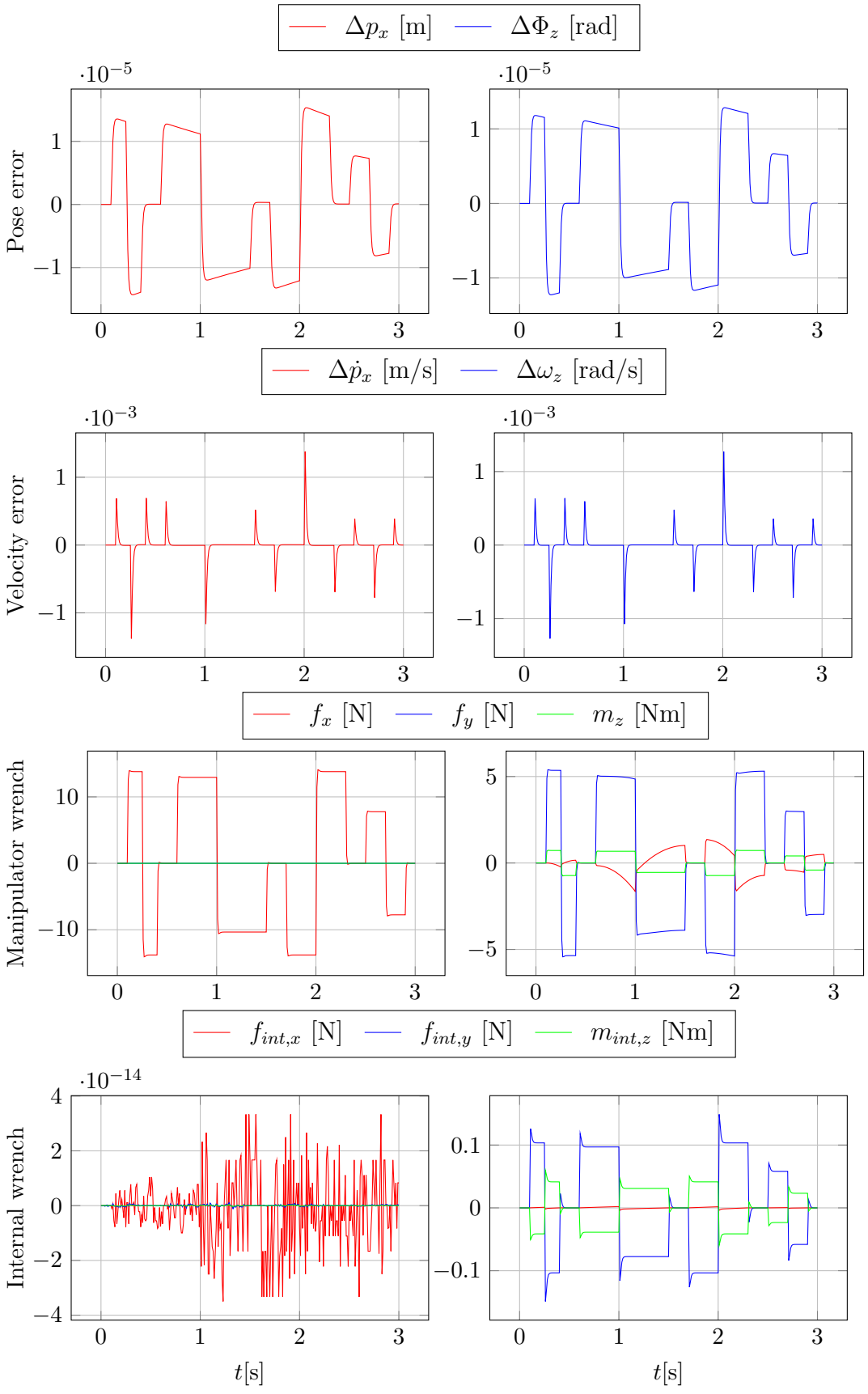

Figure 4.3: Internal impedance control with feed-forward of the object dynamics: Translation (left column) and rotation

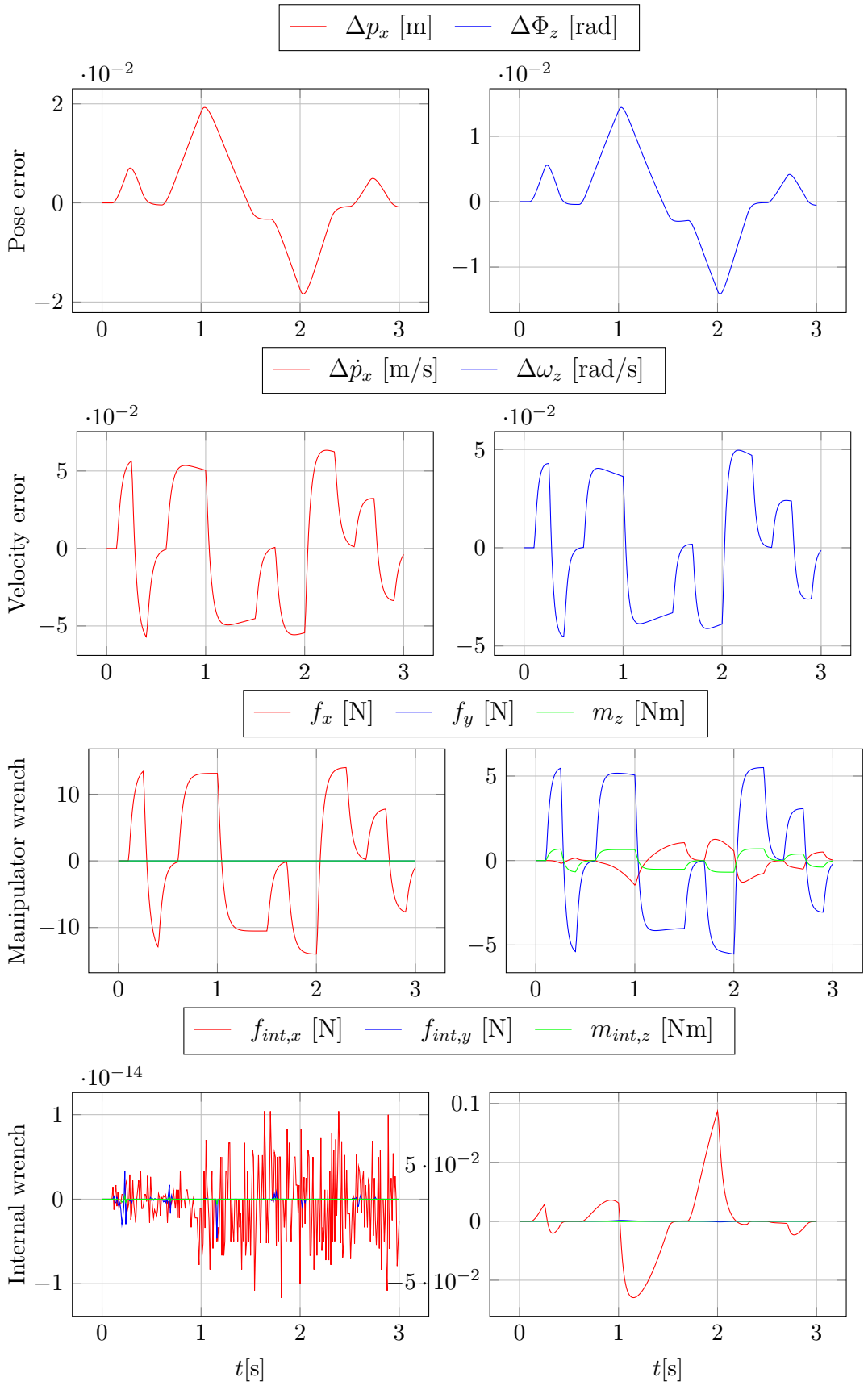

Figure 4.5: Dynamic IPC: Translation (left column) and rotation

Table 4.5: Parameters for the constrained dynamic IPC

	linear	angular
Virt. object inertia	$1.4\text{kg} \cdot I_3$	$0.2\text{kgm}^2 \cdot I_3$
Virt. manipulator inertia	$0.5\text{kg} \cdot I_3$	$0.25\text{kgm}^2 \cdot I_3$
Ext. damping	$1500\text{kg/s} \cdot I_3$	$1500\text{kgm}^2/\text{s} \cdot I_3$
Ext. stiffness	$700\text{N/m} \cdot I_3$	$700\text{Nm} \cdot I_3$
Int. damping	$900\text{kg/s} \cdot I_3$	$45\text{kgm}^2/\text{s} \cdot I_3$
Int. stiffness	$180\text{N/m} \cdot I_3$	$9\text{Nm} \cdot I_3$

4.2 Simulation of the constrained dynamics IPC

The implementation of the constrained dynamics IPC as proposed in section 2.6 does not suffer from numerical issues as the classic IPC. This allows to increase the angular stiffness and damping and achieve a better dynamic performance for an angular motion. The simulation results are shown in figure 4.6. Note that including the inertias of the manipulators in the controller introduces further energy storing elements, i.e. makes the controller more inert. The better trajectory tracking (especially in angular motion) in comparison to the classic IPC results from the higher parameters, which are reported in table 4.5. By choosing the controller manipulator inertia lower than in the robotic system the dynamic response can be improved. The angular velocity deviation is halved in comparison to the classic IPC, but still approximately 20 times higher than in the impedance control approaches. All controllers are tuned to command the same magnitude of force to the robots, the deviations in tracking behaviour result from different force gradients.

4.3 Compliant trajectory generating IPC

The compliant trajectory generating IPC uses an force control loop to compute the force commands for the robots. The structure can either be viewed as PI-control or as a spring and a damper in parallel. Gains or stiffness/damping can be chosen high because the superimposed control scheme already establishes compliance [CCMV08]. The simulation settings are summarized in table 4.6. Numerical stability problems also occur with this approach, damping and stiffness cannot be chosen as high as for in the previous simulations. The parameters reported in table 4.6 are chosen as high as possible to achieve numerical stability with a fixed step solver (*ode8*) at 1 ms step size. A variable step solver (e.g. *ode45*) is stable with higher stiffness and damping and performance is superior. Due to non-applicability in real robotic system, variable-step solvers are not considered further. Although the chosen stiffness and damping is still comparable to the classic IPC parameters, the dynamic performance is inferior because of the additional inertias, which have to be accelerated. This results in approx. double errors in position/orientation and

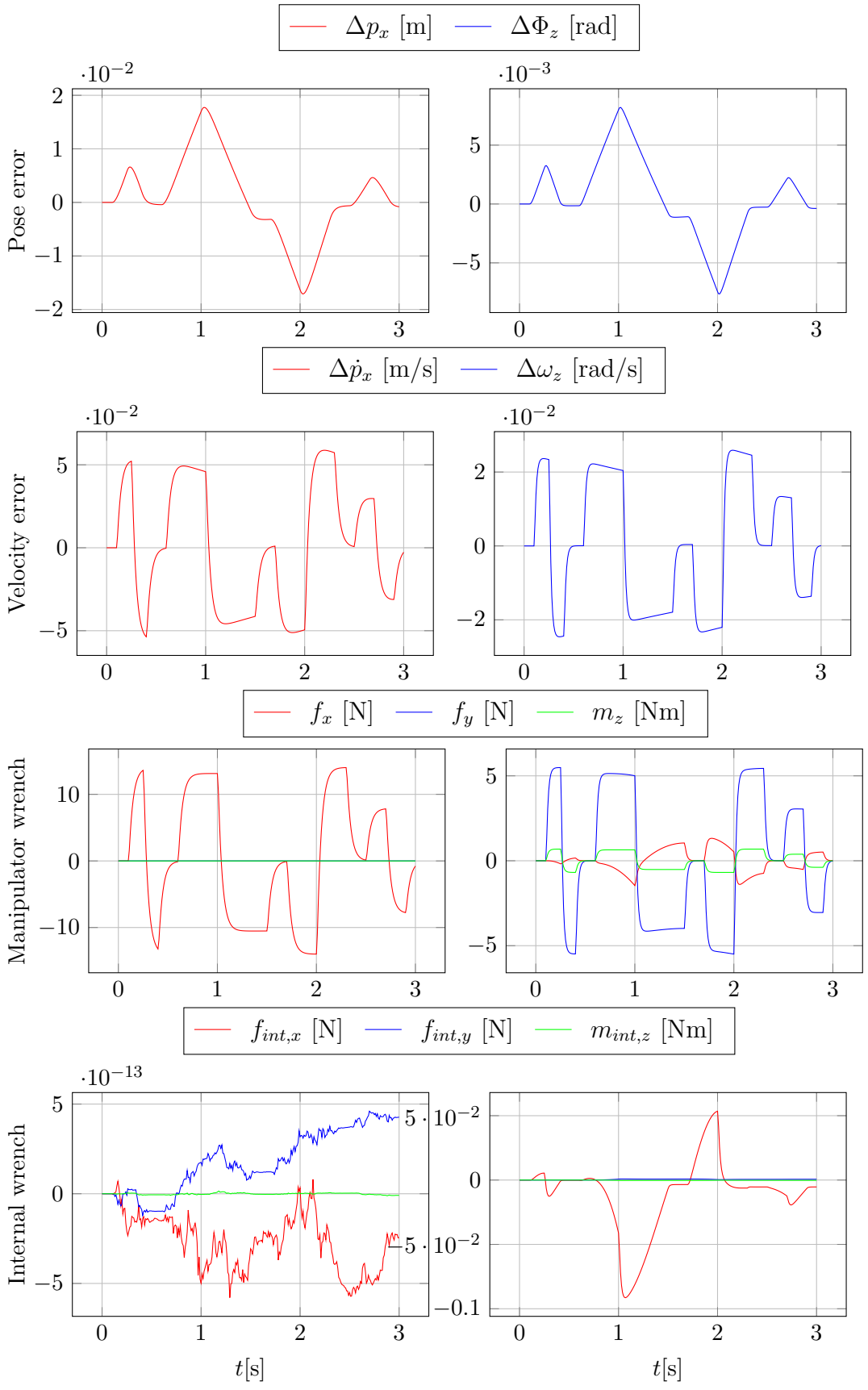

Figure 4.6: Constrained dynamic IPC: Translation (left column) and rotation

Table 4.6: Parameters for the compliant trajectory generating IPC

	linear	angular
Virt. object inertia	$1.4\text{kg} \cdot I_3$	$0.2\text{kgm}^2 \cdot I_3$
Virt. manipulator inertia	$10\text{kg} \cdot I_3$	$0.5\text{kgm}^2 \cdot I_3$
Ext. damping	$1500\text{kg/s} \cdot I_3$	$500\text{kgm}^2/\text{s} \cdot I_3$
Ext. stiffness	$700\text{N/m} \cdot I_3$	$400\text{Nm} \cdot I_3$
Int. damping	$600\text{kg/s} \cdot I_3$	$30\text{kgm}^2/\text{s} \cdot I_3$
Int. stiffness	$120\text{N/m} \cdot I_3$	$6\text{Nm} \cdot I_3$
Force control damping	$5000\text{kg/s} \cdot I_3$	$1500\text{kgm}^2/\text{s} \cdot I_3$
Force control stiffness	$500\text{N/m} \cdot I_3$	$200\text{Nm} \cdot I_3$

velocity compared to the classic IPC (see figure 4.7). In contrast to the constrained dynamic IPC the virtual inertias for the object and the manipulators cannot be chosen smaller than their real pendants. Doing so leads to infinite simulation results. This entails in an even wider performance gap to the constrained dynamic IPC.

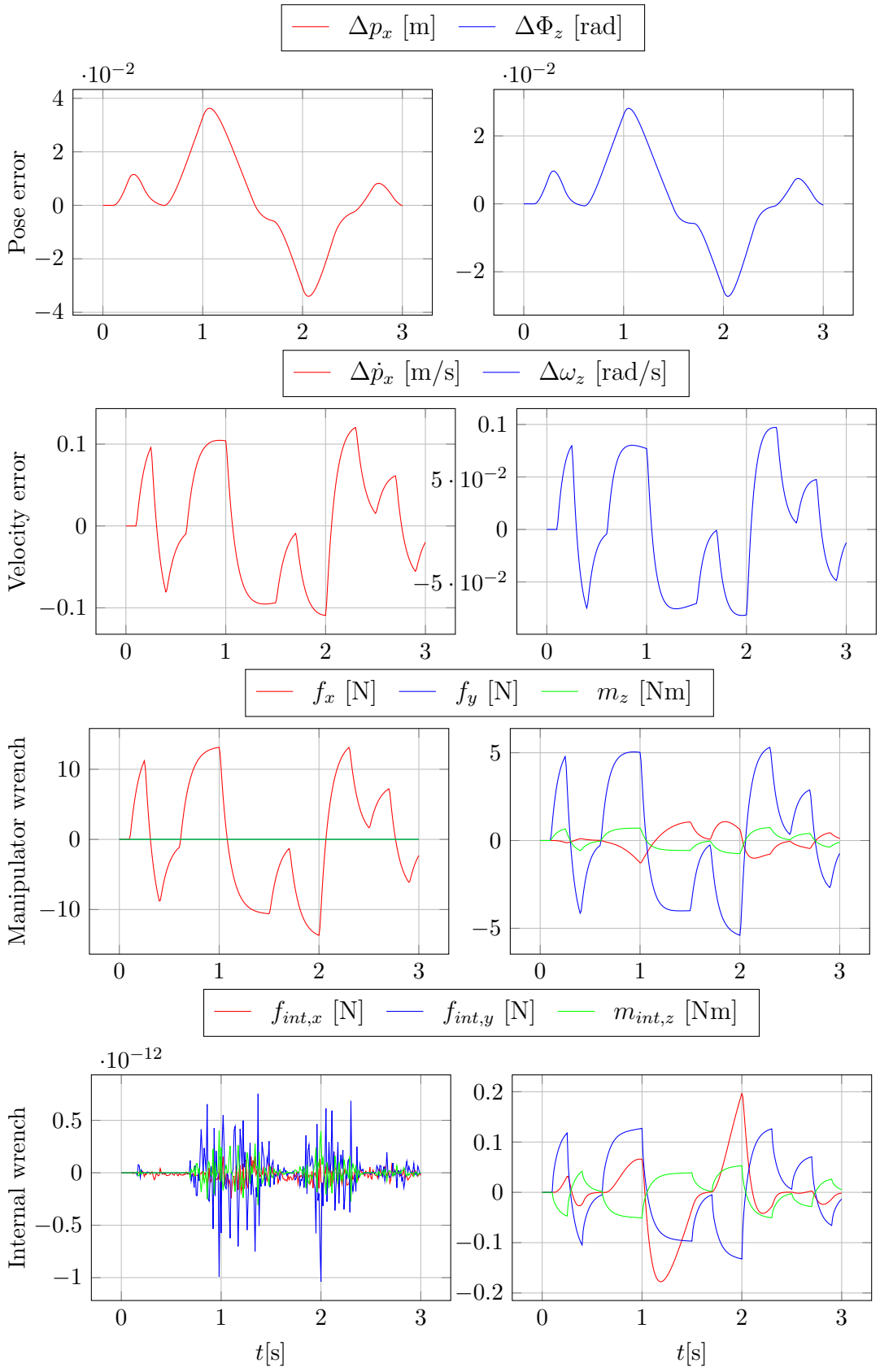

Figure 4.7: Compliant reference trajectory generating IPC: Translation (left column) and rotation

4.4 Energy-bounded trajectory tracking

In the presented simulation, trajectory tracking demands more energy than is available from the energy tank (detailed in section 3.2). The budget for performing operations is limited to 30 J, in accordance with the safety limit of neck fractures (see section 3.1). Trajectories exceeding this limit are adapted with the variable stiffness and damping technique presented in subsection 3.2.1. The underlying control scheme is the dynamic constrained IPC from section 2.6.
In the simulation no energy is lost in the robotic system (due to friction or work on the environment). If the user commands acceleration, energy is transferred from the tank through the controller into the robotic system and is thereby stored in form of potential and energy. When the system slows down, the kinetic and potential energy is is re-transformed into free energy and stored in the tank. This happens in an ideal, lossless way, thus the energy tank reaches the former level after an operation (see the third plot in figure 4.8). Upon depletion of the tank (approx. at $t = 2$ s), the kinetic energy cannot be further increased and the velocity stays constant (observable from the second plot). The reduction of the stiffness and the damping starts as soon as the level falls under a certain threshold, here $T_{th} = 10$ J. As a consequence from $t = 1.7$ s on the velocity increases slower. The actual position falls behind the desired (first plot in figure 4.8). With the reduced velocity it takes until $t = 2.6$ s to catch up to the desired position. During this time the velocity is kept at the energetically feasible maximum. As soon as the velocity reduces the energy level recovers quickly. The approach attempts optimal position tracking under the given energy constraint and no permanent deviations occur after the energetic level has recovered.

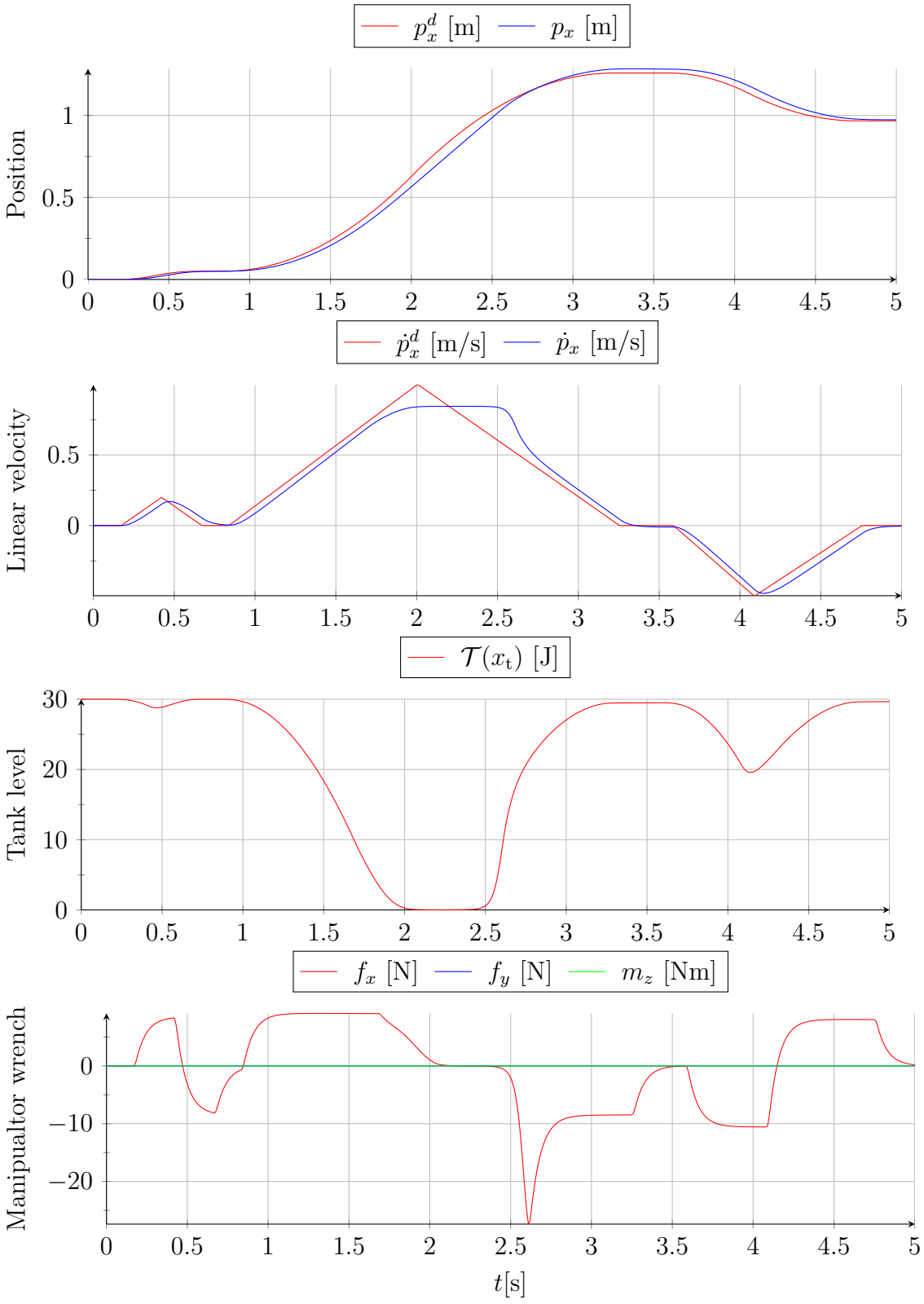

Figure 4.8: Energy bounding by a variable stiffness spring and a variable damper

Chapter 5

Conclusion

Cooperative manipulation is analysed for the first time in the port-Hamiltonian setting. The port-Hamiltonian formulation allows to design a model-based controller by interconnecting atomic mechanical elements and facilitates passivity-based control. It is shown how the modelling of a cooperative set-up transfers into a virtual structure to control the formation of robots. In modelling, a special focus is on the rigid connection of manipulators and object. This constrained contact situation is common in cooperative manipulation. In contrast to [EH16], this thesis provides a self-contained derivation of the internal forces that arise from the constraints. It is shown that these forces do not generate, store or dissipate energy, i.e. a rigid connection is energy consistent. The modelling of the rigid connections is also used for control.
Two model-based controllers are designed for the teleoperated, shared control task of cooperative object manipulation. They use a virtual structure built from springs, masses and dampers to achieve a desired group behaviour of the robots. The design is based on physical intuition and is intrinsically passive. The two proposed controllers differ in terms of their output variables, one generates a compliant reference trajectory for each robot and the other issues force commands to the robots. In the simulative study the force-output controller performs better because the trajectory-generating one suffers from numeric instabilities.
The proposed control design is validated by simulative comparison against cooperative manipulation control schemes known from literature. Impedance control approaches show better dynamic behaviour but achieve stability with a more limited class of environments. The dynamic IPC by Wimböck et al. [WOH08] is passive and has an architecture similar to the proposed controllers. To allow for a comparison with the proposed approaches, it is extended to six DoF and simulated. The results compare well. Internal forces indicate how well a controller preserves the formation of the robots. All simulated approaches show internal forces close to zero, i.e. good coordination performance. The simulation results await experimental validation in a future study.
The proposed schemes are designed for shared control, i.e. involve the human in

the control loop. Humans are commonly considered fail-safe in teleoperation. This is the first work to consider stability and safety issues with non-reactive interfaces. The human is virtually coupled by a spring and a damper to the system. The model-based control design on energy level allows to identify potentially harmful energy in the system. The controller relaxes the coupling of the human, if an unsafe state is detected. The adaptive coupling then prevents the human from supplying further energy to the system. An energy tank is used to passivate the coupling. Simulation results validate the effectiveness of the proposed energy bounding.
Asymptotic stability is ensured by the passive controller for finite energy supplies. For human commands that require infinite energy for execution, the energy-bounding still achieves stability.
Limiting the energy also restricts the possible impact in case of a collision with a human or the environment and thus enhances safety. The prime task in cooperative manipulation is the transportation of large and/or heavy objects, usually this is carried out at low speeds. Injuries due to violent pressure on a clamped human may be more relevant in this set-up. The proposed energy shaping approach also limits the possible force. Suitable safety metrics for violent pressure should be identified from literature and implemented in a continuative study. With the focus on safety, a natural extension of this work is to consider direct human-robot team interaction under the leader-follower paradigm. Also for indirect human-robot interaction, i.e. teleoperation over non-restrictive interfaces, work remains to be done. This thesis examines safety and stability in the shared control of a robot team. A generalization of the energy shaping approach to a wider class of telerobots, controlled with non-restrictive interfaces, is conceivable.

List of Figures

Bibliography

[BH96] R.G. Bonitz and T.C. Hsia. Internal force-based impedance control for cooperating manipulators. *IEEE Transactions on Robotics and Automation*, 12(1):78–89, Feb 1996. doi:10.1109/70.481752.

[CCMV08] F. Caccavale, P. Chiacchio, A. Marino, and L. Villani. Six-dof impedance control of dual-arm cooperative manipulators. *IEEE/ASME Transactions on Mechatronics*, 13(5):576–586, 2008. doi:10.1109/TMECH.2008.2002816.

[CM08] F. Caccavle and Uchiyama M. Cooperative manipulation. In Bruno Siciliano and Oussama Khatib, editors, *Springer Handbook of Robotics*, chapter 29, pages 701–718. Springer, 2008. doi:10.1007/978-3-540-30301-5.

[CV01] F. Caccvale and L. Villani. An impedance control strategy for cooperative manipulation. In *Proc. IEEE/ASME Int. Conf. on Advanced Intelligent Mechatronics*, volume 1, pages 343–348, 2001. doi:10.1109/AIM.2001.936478.

[DMSB09] V. Duindam, A. Macchelli, S. Stramigioli, and H. Bruyninckx. *Modeling and Control of Complex Physical Systems*. Springer, 2009. doi:10.1007/978-3-642-03196-0.

[DS09] V. Duindam and S. Stramigioli. *Modeling and Control for Efficient Bipedal Walking Robots*, volume 53 of *Springer Tracts in Advanced Robotics*. Springer, 2009. doi:10.1007/978-3-540-89918-1.

[EH16] S. Erhart and S. Hirche. Model and analysis of the interaction dynamics in cooperative manipulation tasks. *IEEE Transactions on Robotics*, 2016.

[FSM+11] M. Franken, S. Stramigioli, S. Misra, C. Secchi, and A. Macchelli. Bilateral telemanipulation with time delays: A two-layer approach combining passivity and transparency. *IEEE Transactions on Robotics*, 27(4):741–756, Aug 2011. doi:10.1109/TRO.2011.2142430.

[GFS+14] G. Gioioso, A. Franchi, G. Salvietti, S. Scheggi, and D. Prattichizzo. The flying hand: A formation of UAVs for cooperative aerial telemanipulation. In *Proc. IEEE Int. Conf. on Robotics and Automation*, pages 4335–4341, May 2014. doi:10.1109/ICRA.2014.6907490.

[Goe52] R.C. Goertz. Fundamentals of general-purpose remote manipulators. *Nucleonics*, 10(11):36–45, 1952.

[GSDLP16] M. Geravand, E. Shahriari, A. De Luca, and A. Peer. Port-based Modeling of Human-Robot Collaboration towards Safety-enhancing Energy Shaping Control. In *Proc. IEEE Int. Conf. on Robotics and Automation*, 2016. accepted for publication.

[Had14] Sami Haddadin. *Towards Safe Robots - Approaching Asimov's 1st Law*, volume 90 of *Springer Tracts in Advanced Robotics*. Springer, 2014. doi:10.1007/978-3-642-40308-8.

[HB12] S. Hirche and M. Buss. Human-oriented control for haptic teleoperation. *Proceedings of the IEEE*, 100(3):623–647, March 2012. doi:10.1109/JPROC.2011.2175150.

[HKDN13] D. Heck, D. Kostic, A. Denasi, and H. Nijmeijer. Internal and external force-based impedance control for cooperative manipulation. In *Proc. European Control Conference*, pages 2299–2304, July 2013.

[Hog84a] Neville Hogan. Adaptive control of mechanical impedance by coactivation of antagonist muscles. *IEEE Transactions on Automatic Control*, 29(8):681–690, Aug 1984. doi:10.1109/TAC.1984.1103644.

[Hog84b] Neville Hogan. Impedance control: An approach to manipulation. In *American Control Conference*, pages 304–313, June 1984.

[Hog89] Neville Hogan. Controlling impedance at the man/machine interface. In *Proc. IEEE Int. Conf. on Robotics and Automation*, pages 1626–1631 vol.3, May 1989. doi:10.1109/ROBOT.1989.100210.

[Ind14] Mitsubishi Heavy Industries. "MEISTeR" Remote Control Robot Completes Demonstration Testing At Fukushima Daiichi Nuclear Power Station, 2014. Press Information 1775, February 20, 2014; Online, accessed January 13, 2016. URL: https://www.mhi-global.com/news/story/1402201775.html.

[LBY03] J. R. T. Lawton, R. W. Beard, and B. J. Young. A decentralized approach to formation maneuvers. *IEEE Transactions on Robotics and Automation*, 19(6):933–941, Dec 2003. doi:10.1109/TRA.2003.819598.

[LH10] D. Lee and K. Huang. Passive-set-position-modulation framework for interactive robotic systems. *IEEE Transactions on Robotics*, 26(2):354–369, April 2010. doi:10.1109/TRO.2010.2041877.

[LL02] G. Liu and Z. Li. A unified geometric approach to modeling and control of constrained mechanical systems. *IEEE Transactions on Robotics and Automation*, 18(4):574–587, Aug 2002. doi:10.1109/TRA.2002.802207.

[LS05] D. Lee and M.W. Spong. Bilateral teleoperation of multiple cooperative robots over delayed communication networks: Theory. In *Proc. IEEE Int. Conf. Robotics and Automation*, pages 360–365, April 2005. doi:10.1109/ROBOT.2005.1570145.

[LTC09] M. Laffranchi, N. G. Tsagarakis, and D. G. Caldwell. Safe human robot interaction via energy regulation control. In *Proc. IEEE/RSJ Int. Conf. on Intelligent Robots and Systems*, pages 35–41, Oct 2009. doi:10.1109/IROS.2009.5354803.

[LTC12] M. Laffranchi, N. G. Tsagarakis, and D. G. Caldwell. Improving safety of human-robot interaction through energy regulation control and passive compliant design. In Maurtua Inaki, editor, *Human Machine Interaction - Getting Closer*, chapter 8, pages 155–170. InTech, 2012. doi:10.5772/1349.

[Mat16] MathWorks. Choose a Solver, 2016. Simulink Documentation R2016a, online, accessed April 23, 2016. URL: http://de.mathworks.com/help/simulink/ug/types-of-solvers.html.

[NPH08] G. Niemeyer, C. Preusche, and G. Hirzinger. Telerobotics. In Bruno Siciliano and Oussama Khatib, editors, *Springer Handbook of Robotics*, chapter 31, pages 741–757. Springer, 2008. doi:10.1007/978-3-540-30301-5.

[OASK+04] C. Ott, A. Albu-Schaffer, A. Kugi, S. Stamigioli, and G. Hirzinger. A passivity based cartesian impedance controller for flexible joint robots - part i: torque feedback and gravity compensation. In *Proc. IEEE Int. Conf. on Robotics and Automation*, volume 3, pages 2659–2665, April 2004. doi:10.1109/ROBOT.2004.1307462.

[OvdSME99] R. Ortega, A. J. van der Schaft, B. Maschke, and G. Escobar. Energy-shaping of port-controlled hamiltonian systems by interconnection. In *Proc. IEEE Conf. on Decision and Control*, volume 2, pages 1646–1651 vol.2, 1999. doi:10.1109/CDC.1999.830260.

[OvdSMM01] R. Ortega, A. J. van der Schaft, I. Mareels, and B. Maschke. Putting energy back in control. *IEEE Control Systems Magazine*, 21(2):18–33, Apr 2001. doi:10.1109/37.915398.

[PST+15] J. R. Peters, V. Srivastava, G. S. Taylor, A. Surana, M. P. Eckstein, and F. Bullo. Human supervisory control of robotic teams: Integrating cognitive modeling with engineering design. *IEEE Control Systems Magazine*, 35(6):57–80, Dec 2015. doi:10.1109/MCS.2015.2471056.

[SC92] S.A. Schneider and R.H. Cannon. Object impedance control for cooperative manipulation: theory and experimental results. *IEEE Transactions on Robotics and Automation*, 8(3):383–394, 1992. doi:10.1109/70.143355.

[SD01] S. Stramigioli and V. Duindam. Variable spatial springs for robot control applications. In *Proc. IEEE/RSJ Int. Conf. on Intelligent Robots and Systems*, volume 4, pages 1906–1911, 2001. doi:10.1109/IROS.2001.976352.

[She92] T.B. Sheridian. *Telerobotcis, Automation and Human Supervisory Control*. MIT Press, Cambridge, 1992.

[SMA99] S. Stramigioli, Claudio Melchiorri, and S. Andreotti. A passivity-based control scheme for robotic grasping and manipulation. In *Proc. IEEE Conf. on Decision and Control*, volume 3, pages 2951–2956, 1999. doi:10.1109/CDC.1999.831385.

[SMH15] D. Sieber, S. Music, and S. Hirche. Multi-robot manipulation controlled by a human with haptic feedback. In *Proc. IEEE/RSJ Int. Conf. on Intelligent Robots and Systems*, pages 2440–2446, Sep 2015. doi:10.1109/IROS.2015.7353708.

[SMP14] S. Scheggi, F. Morbidi, and D. Prattichizzo. Human-robot formation control via visual and vibrotactile haptic feedback. *IEEE Transactions on Haptics*, 7(4):499–511, Oct 2014. doi:10.1109/TOH.2014.2332173.

[Str01a] Stefano Stramigioli. Geometric modeling of mechanical systems for interactive control. In Alfonso Banos, Francoise Lamnabhi-Lagarrigue, and Francisco J. Montoya, editors, *Advances in the control of nonlinear systems*, volume 264 of *Lecture Notes in Control and Information Sciences*, pages 309–332. Springer, 2001. doi:10.1007/BFb0110375.

[Str01b] Stefano Stramigioli. *Modeling and IPC Control of Interactive Mechanical Systems: A Coordinate-Free Approach*, volume 266 of *Lecture Notes in Control and Information Sciences*. Springer, 2001. doi:10.1007/BFb0110400.

[Str15] Stefano Stramigioli. Energy-aware robotics. In M. K. Camlibel, A. A. Julius, R. Pasumarthy, and J. Scherpen, editors, *Mathematical Control Theory I*, volume 461 of *Lecture Notes in Control and Information Sciences*, pages 37–50. Springer, 2015. doi:10.1007/978-3-319-20988-3.

[TASLH08] L. Le Tien, A. Albu-Schaffer, A. De Luca, and G. Hirzinger. Friction observer and compensation for control of robots with joint torque measurement. In *Proc. IEEE/RSJ Int. Conf. on Intelligent Robots and Systems*, pages 3789–3795, Sept 2008. doi:10.1109/IROS.2008.4651049.

[TdVS14] T. S. Tadele, T. J. A. de Vries, and S. Stramigioli. Combining energy and power based safety metrics in controller design for domestic robots. In *2014 IEEE International Conference on Robotics and Automation (ICRA)*, pages 1209–1214, May 2014. doi:10.1109/ICRA.2014.6907007.

[vdS06] Arjan J. van der Schaft. Port-hamiltonian systems: an introductory survey. In M. Sanz-Sole, J. Soria, J.L. Varona, and J. Verdera, editors, *Proc. Int. Congress of Mathematicians Vol. III: Invited Lectures*, pages 1339–1365, Madrid, Spain, 2006. European Mathematical Society Publishing House.

[vdS13] Arjan J. van der Schaft. Port-hamiltonian differential-algebraic systems. In A. Ilchmann and T. Reis, editors, *Surveys in Differential-Algebraic Equations I*, pages 173–226. Springer, 2013. doi:10.1007/978-3-642-34928-7.

[vdSJ14] A. J. van der Schaft and Dimitri Jeltsema. *Port-Hamiltonian Systems Theory: An Introductory Overview*. Foundations and Trends in Systems and Control. NOW Publishing Inc., Hanover, MA, 2014. doi:10.1561/2600000002.

[VSvdSP14] Ewoud Vos, Jacquelien M.A. Scherpen, A. J. van der Schaft, and Ate Postma. Formation control of wheeled robots in the port-hamiltonian framework. In *World Congress of the International Federation of Automatic Control (IFAC)*, volume 19, pages 6662–6667, 2014. doi:10.3182/20140824-6-ZA-1003.00394.

[WOH06] T. Wimboeck, C. Ott, and G. Hirzinger. Passivity-based object-level impedance control for a multifingered hand. In *Proc. IEEE/RSJ Int. Conf. on Intelligent Robots and Systems*, pages 4621–4627, Oct 2006. doi:10.1109/IROS.2006.282170.

[WOH08] T. Wimboeck, C. Ott, and G. Hirzinger. Analysis and experimental evaluation of the intrinsically passive controller (ipc) for multifingered hands. *Porc. IEEE Int. Conf. on Robotics and Automation*, pages 278–284, May 2008. doi:10.1109/ROBOT.2008.4543221.

[Woo71] Jack L. Wood. Dynamic response of human cranial bone. *Journal of Biomechanics*, 4(1):1 – 12, 1971. doi:10.1016/0021-9290(71)90010-8.

[WS08] K. Waldron and J. Schmiedeler. Kinematics. In Bruno Siciliano and Oussama Khatib, editors, *Springer Handbook of Robotics*, chapter 1, pages 9–33. Springer, 2008. doi:10.1007/978-3-540-30301-5.

[YPM+96] N. Yoganandan, F.A. Pintar, D.J. Maiman, J.F. Cusick, A. Sances, and P.R. Walsh. Human head-neck biomechanics under axial tension. *Medical Engineering and Physics*, 18(4):289 – 294, June 1996. doi:10.1016/1350-4533(95)00054-2.

License